# Sumatra's Endemic Crested Dragons (Agamidae: Lophocalotes): A New Species from the Bukit Barisan Range, Comments on Lophocalotes ludekingi, and Ecology

**Article** *in* Herpetologica · March 2018

DOI: 10.1655/Herpetologica-D-17-00022.1

CITATIONS
0

READS
733

**6 authors**, including:

Michael B Harvey
Broward College
**74** PUBLICATIONS **956** CITATIONS
SEE PROFILE

James Scrivani
Oregon State University
**1** PUBLICATION **0** CITATIONS
SEE PROFILE

Kyle J Shaney
Universidad Nacional Autónoma de México
**24** PUBLICATIONS **293** CITATIONS
SEE PROFILE

Amir Hamidy
Indonesian Institute of Sciences
**144** PUBLICATIONS **497** CITATIONS
SEE PROFILE

*Herpetologica*, 74(1), 2018, 73–88


# Sumatra's Endemic Crested Dragons (Agamidae: *Lophocalotes*): A New Species from the Bukit Barisan Range, Comments on *Lophocalotes ludekingi*, and Ecology

Michael B. Harvey[1,6], James Scrivani[1,5], Kyle Shaney[2], Amir Hamidy[3], Nia Kurniawan[4], and Eric N. Smith[2]

[1] Department of Biological Sciences, Broward College, 3501 Southwest Davie Road, Davie, FL 33314, USA
[2] The Amphibian and Reptile Diversity Research Center and Department of Biology, University of Texas at Arlington, 501 South Nedderman Drive, Arlington, TX 76010, USA
[3] Laboratory of Herpetology, Museum Zoologicum Bogoriense, Research Center for Biology, Indonesian Institute of Sciences—LIPI, Jl Raya Jakarta Bogor km 46, Cibinong, West Java 16911, Indonesia
[4] Department of Biology, Universitas Brawijaya, Jl Veteran, Malang, East Java 65145, Indonesia

Abstract: With the use of a concordance and a mitochondrial tree–morphological character congruence approach, we show that recently discovered populations of *Lophocalotes* represent a new species. Like its only known congener, the new species occurs only on Sumatra in montane forests above 1000 m. The new species differs from *L. ludekingi* in having more gulars, ventrals, and subdigital lamellae; in having males with a lower nuchal crest not supported by an arched flap of skin and white gular markings; and in having females with cream buccal epithelia. These agamids are slow-moving, arboreal, generalist predators and lay 2–6 eggs, multiple times per year. *Lophocalotes* exhibits pronounced sexual dimorphism. Interestingly, coloration of the buccal epithelium is sexually dichromatic in the new species. The recently described nematode *Spinicauda sumatrana* infected most hosts in our sample, and parasite load increased with snout-to-vent length. *Lophocalotes* is closely related to *Dendragama* and *Pseudocalotes* and shares two derived characters with *Pseudocophotis sumatrana*: a prehensile tail and reduced keels on the subdigital lamellae.

**Key words:** Clutch size; Diet; *Lophocalotes achlios* sp. nov.; ND4; Parasites; Sexual dimorphism; *Spinicauda sumatrana*; Systematics

In the minutes of the Koninklijke Natuurkundige Vereeniging in Nederlandsch Indië, reporting various events in Sumatra and Java, Bleeker (1860) described new lizards from Agam on the slopes of Mount Singgalang, West Sumatra, Indonesia. His accounts included the description of *Calotes ludekingi*, which he named in honor of the Dutch physician E.W.A. Lüdeking, a collector for the Rijksmuseum van Natuurlijke Historie, Leiden. However, this small collection would not be housed in Leiden. Instead, in 1863, the British Museum acquired the collection, including Bleeker's type specimen. Apparently unaware of Bleeker's publication, Günther (1872) described the same specimen as a new genus and species, *Lophocalotes interruptus*. Günther's new name appeared in Boulenger's (1885) Catalogue of Lizards in the British Museum, and remained in use until Hubrecht (1887) suspected that Bleeker's species might be the same as Günther's. Boulenger (1887) definitively corrected Günther's mistake.

Bleeker's (1860) brief description of the holotype mentions the hypertrophied jaw muscles, color pattern on the neck, and scales on the neck being much larger than those on the belly. He did not make comparisons with any other agamids, however, and his description does not distinguish his new species from other Sumatran draconines. Günther (1872:593) provided an illustration of the type specimen and differentiated his new genus from *Calotes* by "the structure of the crest, which is interrupted on the neck, and formed by distant spines on the back." Later, Boulenger (1885) observed that the subdigital lamellae of *Lophocalotes* lack keels and used this distinctive diagnostic character in his key to agamid genera.

Specimens of *Lophocalotes ludekingi* remain rare in collections. Manthey and Grossmann (1997) provided a modern description of this species. Hallermann et al. (2004) reported it from Jambi, described coloration in life, published color photographs of several recently collected specimens, and reported limited mensural and meristic data for 16 specimens in the RMNH, ZFMK, and ZISP (institutional abbreviations follow Sabaj 2016). They found no differences between specimens from the type locality and those in Jambi, concluding that both populations belong to the same species.

In 2013, we began an inventory of reptiles and amphibians across Sumatra (Harvey et al. 2014, 2016, 2017a,b; Smart et al. 2017). During this survey, we discovered new populations of *Lophocalotes* 150 km to the south of the known range of *L. ludekingi*. In the field, we noted subtle differences between the northern and southern populations. Herein, we investigate the taxonomic status of these southern populations and describe several aspects of their ecology.

## Materials and Methods

### Fieldwork

Teams of researchers from Broward College (BC), the Museum Zoologicum Bogoriense (MZB), the Universitas Brawijaya (UB), and the University of Texas at Arlington (UTA) conducted surveys mostly along trails and streams through montane forests, cultivated areas, and areas of secondary growth during June and July 2013, and July and August 2015. We conducted most surveys at night and recorded GPS coordinates (in all cases, datum = WGS84). We photographed specimens in life, euthanized them with benzocaine, and stored either liver or muscle in 1.5 ml of cell lysis buffer for DNA extraction. The lizards were fixed in

[5] Present Address: Department of Forest Engineering, Resources, and Management, College of Forestry, Oregon State University, Corvalis, OR 97331, USA.
[6] Correspondence: e-mail, mharvey@broward.edu

10% formalin, and transferred to 70% ethanol for permanent storage at the MZB and UTA. We everted hemipenes of most males in the field and sexed the remaining specimens by ventral incisions. Before fixing, we weighed each specimen with a digital balance (±1 g). We placed each specimen on a flat surface next to a ruler and took photographs of the dorsal, lateral, and ventral sides. For selected specimens, we also made multiple photos of live animals in natural settings. We deposited photos of all specimens at UTA.

## Morphological Data

We scored each specimen for a suite of meristic, mensural, and qualitative characters that have proven useful for diagnosing and describing lizards in the closely related genera *Dendragama* (Harvey et al. 2017a) and *Pseudocalotes* (Harvey et al. 2014, 2017b).

We measured the following traits with a ruler (± 1 mm): snout–vent length (SVL, from the tip of the snout to the anterior lip of the cloaca), body length (from the posterior insertion of the arm to the anterior insertion of the leg), pectoral width (axilla to axilla), and length of the tail (from the posterior lip of the cloaca). With a digital caliper (± 0.1 mm), we measured tail height and width immediately behind the swollen skin surrounding the cloaca. When measuring the height of the tail, we placed the caliper on the proximal end of any projecting vertebral scale so that the projecting distal end was not included in the measurement.

We measured Fingers III and IV and Toes IV and V by pressing the digits to a flexible ruler and measuring from the interdigital skin to the base of the claw. With digital calipers (± 0.1 mm), we measured head length (from the occiput to the center of the snout), distance from the anterior border of the auditory meatus to the center of the snout, head width (at the rictus), maximum diameter of the orbit (bony edge to bony edge; we took this measurement along a line parallel to the ocular aperture, because the orbit is widest along this line), shortest distance from the posterior border of the orbit to the anterior margin of the auditory meatus, length of the tympanic membrane, width of the snout (between the upper margins of the nostrils), greatest width and height of the rostral, length of the shank (from the center of the knee to the preaxial base of Toe I), height of the longest nuchal crest scale (a straight-line measure from the anteriormost edge of the scale to its apex), and height of the longest dorsal crest scale (same technique as for nuchal crest scales).

For characters that could be scored on either side of the body (i.e., bilateral characters) such as length of the shank and counts of labials, we scored meristic characters on the left side and mensural characters on the right side of each specimen. When a bilateral character could not be scored on one side, we switched sides.

A few characters used in this study require further comment. *Lophocalotes* has a greatly enlarged lorilabial just below and behind the eye (Fig. 1). This scale overlies the rictus, and the posterior border of the last supralabial shares a suture with this scale. The last infralabial is the scale positioned directly below the center of the last supralabial. We identified the last canthal as a scale ending directly above or extending beyond a straight vertical line at the anterior margin of the orbit. We counted circumorbitals by the method of Harvey et al. (2014), and transorbitals as the number of scales in a transverse line between, but not including, the last supraciliary scales. Our transorbital count is identical to the "Head Scales: HeadStr" character defined by Zug et al. (2006). Counts of subdigital lamellae include all scales from the interdigital skin to the claw and include the elongate ungual scale. We followed the terminology of Harvey et al. (2014, 2017a,b) for scales of the neck and flanks. When counting vertebral scales, we used the same methods as in our recent revision of *Dendragama* (Harvey et al. 2017a) and only include projecting scales in the count. However, we distinguished lanceolate scales of the nuchal crest from several smaller triangular crest scales that separate the occiput from the lanceolate crest scales.

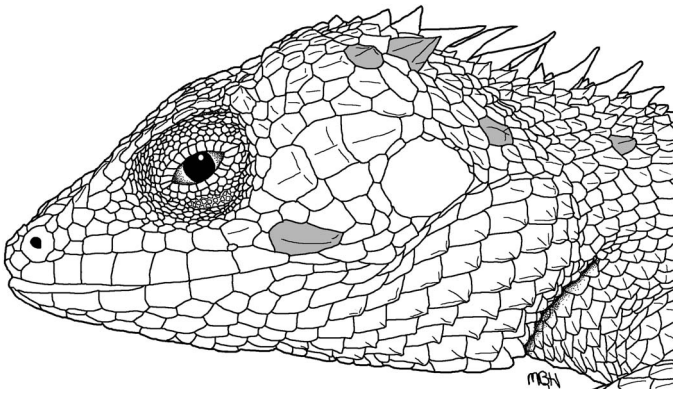

FIG. 1.—Cephalic morphology of *Lophocalotes achlios* (holotype, length of head from occiput to rostral = 22.4 mm). Scales shaded for emphasis are the greatly enlarged lorilabial marking location of rictus; single modified scale of dorsolateral series on neck; and temporal, posttemporal, and posttympanic modified scales.

We counted bands on the body and tail from pictures taken in the field, because banding faded in some specimens after preservation. On the tail, small oval blotches are positioned in the interspaces. These are not included in the count of caudal bands. In about one-half of the specimens from Dempo, caudal bands could not be counted because of fracturing of bands, fading, or darkening on the distal tail.

## Species Concept, and Delineation

We view species as separately evolving metapopulations and agree with de Queiroz's (1998) observation that many, if not all, contemporary species concepts are special cases of the general lineage concept. Operationally, we recognize allopatric populations as species when we find concordance (Avise and Ball 1990) of multiple, apparently independent characters. For this study, we employ the "mitochondrial tree–morphological character congruence" approach of species delineation as defined by Miralles and Vences (2013; also see Miralles et al. 2016). Accordingly, we recognize species as monophyletic clades sharing suites of apparently fixed molecular and morphological characters. Geographic isolation of the clades and exclusivity (sensu Wiens and Penkrot 2002) provides additional evidence of interrupted gene flow.

## Mitochondrial DNA Sequences and Phylogenetic Analysis

We extracted genomic DNA from muscle or liver tissue taken from eight specimens of *Lophocalotes*, including individuals from each sampled locality. For phylogenetic

TABLE 1.—Accession numbers and locality data for specimens used in the molecular analyses.

| Species | Museum number | Locality | GenBank sequence accession number |
|---|---|---|---|
| *Bronchocela cristatella* | UTA 62895 | Ngarip, Lampung, 5.30638°S, 104.5483°E | KT180148 |
| *Dendragama australis* | MZB 13784 | Gunung Dempo, Sumatera Selatan, 4.0422°S, 103.14874°E | KY576740 |
| *D. boulengeri* | MZB 13818 | Gunung Marapi, Sumatera Barat, 4.03744°S, 103.14526°E | KY576742 |
| *Lophocalotes ludekingi* | UTA 62841 | Gunung Kerinci, Jambi, 1.74717°S, 101.2593°E | MF774068 |
| *L. ludekingi* | MZB 14044 | Gunung Kerinci, Jambi, 1.74717°S, 101.25935°E | MF774067 |
| *L. ludekingi* | UTA 62846 | Gunung Kerinci, Jambi, 1.7404°S, 101.25974°E | MF774066 |
| *L. ludekingi* | UTA 62848 | Gunung Tujuh, Jambi, 1.70974°S, 101.37089°E | MF774069 |
| *L. achlios* | UTA 63729 | Gunung Kaba, Bengkulu, 3.50079°S, 102.63513°E | MF774063 |
| *L. achlios* | UTA 63735 | Gunung Kaba, Bengkulu, 3.50757°S, 102.62927°E | MF774064 |
| *L. achlios* | MZB 14040 | Gunung Dempo, Sumatera Selatan, 4.04065°S, 103.14792°E | MF774065 |
| *L. achlios* | UTA 63726 | Gunung Patah, Sumatera Selatan, 4.2273°S, 103.41586°E | MF774062 |
| *Pseudocalotes cybelidermus* | UTA 60551 | Gunung Pesagi, Sumatera Selatan, 4.90149°S, 104.13401°E | KT180139 |
| *P. cybelidermus* | UTA 60549 | Gunung Pesagi, Sumatera Selatan, 4.90711°S, 104.1348°E | KT180140 |
| *P. guttalineatus* | UTA 60540 | Mountain above Ngarip, Sumatera Selatan, 5.28105°S, 104.56183°E | KT180141 |
| *P. guttalineatus* | UTA 60501 | Gunung Pesagi, Sumatera Selatan, 4.90681°S, 104.13457°E | KT180142 |

analysis, we selected sequences of five other agamids and used *Bronchocela cristatella* to root the tree. We chose outgroup taxa based on the phylogenetic analysis of Harvey et al. (2017b), and we provide GenBank numbers for all specimens (Table 1).

We sequenced a fragment of the NADH dehydrogenase subunit 4 (ND4) gene with the use of the forward primer 5′CACCTATGACTACCAAAAGCTCATGTAGAAGC-3′(ND4) and reverse primer 5′CATTACTTTTAC TTGGATTTGCACCA-3(LEU), which targeted an 892–base-pair (bp) region of the gene (Harvey et al. 2014, 2017b). The ND4 thermal cycle profile consisted of an initial denaturation at 94°C for 3 min, followed by 30 cycles of denaturation at 94°C for 30 s, a 50°C annealing phase for 45 s, and a 72°C extension for 1 min, followed by a 72°C extension for 7 min, then a holding phase at 4°C. We cleaned the products of amplification with the use of Sera-Mag Speedbeads (Fisher Scientific, Pittsburgh, PA, USA), following the procedure outlined by Rohland and Reich (2012).

We sequenced polymerase chain reaction (PCR) products with both primers with Sanger sequencing technology. To edit sequences, we used Sequencher v5.4.6 (Gene Codes Corporation, Ann Arbor, MI, USA). We aligned all sequences with the use of the ClustalW alignment setting implemented within Geneious (v6.1.8; Kearse et al. 2012). We checked all alignments for stop codons by eye and trimmed them to equal lengths to remove missing data. Trimmed ND4 sequences in our analysis contained 588 bp.

We selected the most likely model of evolution for each codon position with Bayesian information criteria implemented in PartitionFinder (Lanfear et al. 2012) for both maximum likelihood (ML) and Bayesian analyses. Based on the results of PartitionFinder, we partitioned by each codon position using GTR + Γ. We conducted maximum likelihood (ML) analyses with the use of raxmlGUI (Stamatakis 2006). We utilized the thorough bootstrapping setting, sampling over 10 runs of 10,000 repetitions, and carried out 20 ML searchers for the best tree. We carried out Bayesian phylogenetic analysis using MrBayes v3.2.1 (Huelsenbeck and Ronquist 2001), and used four independent runs (nruns = 4) and four chains (three heated chains and one cold chain) for 10 million generations, sampling every 100 generations. Default temperatures for chains were used. We confirmed adequate mixing and assessed the appropriate amount of burn-in and convergence by inspecting the log files in the program TRACER (v1.6, Baysian Evolutionary Analysis Sampling Trees [BEAST]) and discarded the first 25% of trees in TreeAnnotator (v2.4.6, BEAST). We conducted UPGMA analyses and calculated uncorrected pairwise distances using MEGA (v5.1; Tamura et al. 2011).

### Statistical Analysis of Morphological Data

We compared our samples of *Lophocalotes ludekingi* from Gunung Kerinci and Gunung Tujuh to two populations of *Lophocalotes* (hereafter referred to as the "Dempo" and "Kaba" populations) in reference to major volcanoes (= gunung berapi) where the populations occur. The Dempo sample includes four specimens from Gunung Dempo and five from Gunung Patah. Approximately 30 km separate these volcanoes, and a mostly unbroken chain of mountains connects them to one another. Similarly, the "Kerinci" sample (Appendix) contains specimens from both Gunung Kerinci and Gunung Tujuh. Fewer than 10 km separate these two mountains and the intervening area consists of a plateau with elevations exceeding 1200 m. Finally, the Kaba sample contains one specimen from the adjacent Gunung Kambing. Fewer than 10 km and a high elevation plateau separate Gunung Kaba and Gunung Kambing.

For meristic characters, we made all pairwise comparisons among the Dempo, Kaba, and Kerinci samples with the use of Tukey's HSD test when samples satisfied the assumptions of normality (verified with the Shapiro–Wilk test) and homogeneity of variance (verified by Levene's test). Having verified these assumptions for each comparison reported, we did not use any nonparametric alternatives to Tukey's test. For characters with only two or three states, we investigated changes in character frequency with the use a two-proportion $z$-test and report Bonferroni-corrected probabilities. We used analysis of covariance (ANCOVA) to test for differences in relative sizes of selected mensural characters with SVL used as a covariate. For the ANCOVAs, we verified the assumption of parallel slopes with an $F$-test.

After establishing species boundaries, we pooled samples to investigate sexual dimorphism further. We assessed sexual dichromatism qualitatively and used statistical methods to test for sexual dimorphism in selected meristic and mensural characters. As for interspecific comparisons, we used ANCOVA for the mensural traits. We verified that our meristic characters satisfied assumptions of homogeneity and

normality, then compared sexes of each species with the use of a Student's *t*-test. We used Welch's nonparametric *t*-test when assumptions were violated. Throughout the description, the range of values is followed by means ± 1 SD in parentheses. We use a solidus (/) to separate left from right counts taken from the same specimen. We used the PAST v3.X statistical software program (Hammer et al. 2001) for all statistical tests.

### Diet Analysis, Collection of Parasites, and Reproductive Biology

We removed the stomach and intestine, opened them longitudinally, and removed any parasites for further study. For the diet analysis, we emptied stomachs into petri dishes, examined them under a stereomicroscope, identified adult insects to order, and identified remaining food items to the smallest taxonomic category possible. With the use of digital calipers (±0.01 mm), we measured length and width of individual prey items, then estimated their volume with the formula for a prolate spheroid ($V = 4/3\pi$[length/2][width/2]$^2$). We found that most ants in the stomach contents were torn apart, although their heads were generally intact. All the ants were about the same size, so we estimated their total volume by counting the heads and multiplying the count by an average of volumes from intact specimens.

We calculated proportional food utilization coefficients ($p_i$) by dividing prey counts in each of the $n$ categories by the total of all prey counts. We then calculated niche breadths using the reciprocal of Simpson's (1949) measure of niche breadth:

$$\text{Niche Breadth} = \frac{1}{\sum_{i=1}^{n} p_i^2}.$$

Niche breadth varies from one (= exclusive use of a single category) to $n$ (= even use of all categories; Pianka 1973, 1986). To compare diets between males and females, we generated a contingency table for the counts of the various food categories. Because several cells in the contingency table contain values less than 5, we report probability of no association with the use of Fisher's exact test. Subscripts of this probability are the degrees of freedom. We did not calculate niche breadths or perform comparisons on volumes, because many prey were heavily masticated and dismembered, complicating our estimates. Nonetheless, we report volumes in our results for descriptive purposes.

The only symbionts recovered from digestive tracts were nematodes and trematodes. We counted the number of nematodes in each specimen, then examined the relationship between parasite load and SVL by linear regression. We tested assumptions of linear regression by using the Durbin–Watson test for positive autocorrelation of residuals in $y$, the Breusch–Pagan test for heteroscedasticity (i.e., nonstationary variance of residuals), and the Shapiro Wilk test for normality of residuals. Residuals from the parasite data were not normally distributed and the Durbin–Watson test was significant. Accordingly, we did not use a *t*-test for the null hypothesis of no correlation. Instead, we report a permutation probability of no correlation generated by PAST (Hammer et al. 2001).

We investigated parasite load and population structure of intestinal helminths by generating a coefficient of dispersion, and by comparing observed parasite counts to those predicted by Poisson and negative binomial models. Based on parameters of the Poisson distribution, a coefficient of dispersion (variance to mean ratio) of parasite counts approaches 1 when parasite loads are random, approaches 0 when they are uniform, and is greater than 1 when parasites are aggregated (Anderson and Gordon 1982). We used the on-line Poisson probability calculator provided by stattrek.com to generate expected Poisson frequencies. To estimate the shape parameter $k$ of the negative binomial, we used the ML approach outlined by Bliss (Bliss and Fisher 1953) and followed his iterative method for calculating expected numbers of hosts for each parasite load. We used Fisher's exact test for goodness of fit between our data and the Poisson and negative binomial model predictions.

We assessed reproductive condition of females by examining ovaries and oviducts on both sides of each specimen. We estimated the volume of oviductal eggs with the formula for a prolate spheroid, $(4\pi/3)a^2c$, where $a$ is the smallest and $c$ is the largest radius of the egg. After verifying assumptions of linearity, homoscedasticity, and normality of residuals, we used linear regression to examine the relationship between SVL, clutch size, and counts of ovarian follicles. We assessed reproductive condition of males by noting degree of coiling and distension of the vasa efferentia.

## Results

### Morphological Comparisons Among Populations

A high, arched flap of skin supports the nuchal crest scales in adult male *Lophocalotes ludekingi* from Kerinci (Fig. 2E), whereas males from Kaba and Dempo lack this flap of skin. In its center, this flap of skin is somewhat taller than the crest scales. Males of *L. ludekingi* have bright yellow–orange scales interspersed among green to bluish-green gular scales (Fig. 2C), whereas males from Kaba and Dempo have white markings on the gulars (Fig. 2D). The yellow–orange gulars contrast with a large white blotch below and behind the tympanum in males from the Kerinci sample. This blotch occurs in all males from Kerinci ($n = 7$) and Dempo ($n = 5$), but in only 20% ($n = 10$) of males from Kaba. The blotch covers 3–20 ($9 \pm 5$, $n = 7$) scales in males from Kerinci and 4–9 ($6 \pm 1$, $n = 5$) scales in males from Dempo. It covers three scales in one male from Kaba and three-quarters of a scale in the other specimen. The remaining males from Kaba (80%, $n = 10$) lack a discrete patch below and behind the ear. Females from the Kaba and Dempo populations lack a patch, whereas 60% of the females from Kerinci have a patch covering 3–5 scales. In the Kerinci population, both males and females have yellow–orange buccal epithelia (Fig. 2B). However, this character is sexually dimorphic in the southern populations: males have yellow–orange buccal epithelia but females have cream epithelia.

Compared to specimens of *Lophocalotes ludekingi* from Kerinci, both southern populations have more gulars, ventrals, and lamellae under Finger IV (Tables 2 and 3; Fig. 3). Comparisons between the Kerinci and Dempo populations were nonsignificant for comparisons between lamellae under Toe IV and between Toe IV lamellae within the span of Toe V (both $P = 0.057$), but the slightly higher probability is likely caused by lower statistical power and small sample sizes. Males from Kerinci develop distinctly


FIG. 2.—Holotype of *Lophocalotes achlios* (A, B, and D; MZB 14038, SVL 90 mm) from Gunung Kaba, Bengkulu Province, Sumatra. Gular region (C, MZB 14044) and nuchal crest (E, MZB 14043) of *L. ludekingi* from Gunung Kerinci, Jambi Province, Sumatra. Dorsal pattern of adult female paratype of *L. achlios* (F, UTA 63732) from Gunung Kaba. Photos by E.N. Smith. A color version of this figure is available on line.

longer nuchal crest scales, and the crest scales appear to lengthen faster during ontogeny (Fig. 3; test for homogeneity of slopes $F_{1,19} = 5.65$, $P = 0.03$; ANCOVA $F_{1,19} = 11.6$, $P = 0.003$) than in males from the southern populations. On average, the Dempo population has more circumorbitals and supralabials than the Kaba population and fewer scales spanning the pectoral gap than either population. The Kaba population has a higher frequency of five postrostrals than the Kerinci population; however, this comparison is only just nonsignificant ($P = 0.059$, following the Bonferroni correction for three comparisons). Although the Kaba population

TABLE 2.—Summary of meristic characters for two species of *Lophocalotes*. Characters found to differ between species ($P < 0.05$) are indicated in boldface type.

| | *Lophocalotes achlios* | | *Lophocalotes ludekingi* |
|---|---|---|---|
| | Kaba population | Dempo population | Kerinci population, Jambi |
| Postrostrals | 3 (0%, $n = 20$) | 3 (9%, $n = 11$) | 3 (9%, $n = 11$) |
| | 4 (40%) | 4 (64%) | 4 (82%) |
| | 5 (50%) | 5 (18%) | 5 (9%) |
| | 6 (0%) | 6 (9%) | 6 (0%) |
| Supranasals | 1 (15%, $n = 20$) | 1 (0%, $n = 11$) | 1 (10%, $n = 10$) |
| | 2 (75%) | 2 (91%) | 2 (70%) |
| | 3 (10%) | 3 (0%) | 3 (20%) |
| | | 4 (9%) | |
| Transorbitals | 12–15 (13 ± 1, $n = 20$) | 10–13 (12 ± 1, $n = 11$) | 8–15 (13 ± 2, $n = 11$) |
| Circumorbitals | 7–11 (9 ± 1, $n = 20$) | 7–9 (8 ± 1, $n = 11$) | 7–10 (9 ± 1, $n = 10$) |
| Supralabials contacting nasal | 1 (85%, $n = 20$) | 1 (64%, $n = 11$) | 1 (64%, $n = 11$) |
| | 2 (15%) | 2 (36%) | 2 (36%) |
| Combined canthals and supraciliaries | 10–13 (11 ± 1, $n = 20$) | 8–11 (10 ± 1, $n = 11$) | 9–13 (11 ± 1, $n = 11$) |
| Loreals separating last canthal from supralabials | 4–7 (5 ± 1, $n = 20$) | 4–6 (5 ± 1, $n = 11$) | 4–6 (5 ± 1, $n = 11$) |
| Loreals between orbit and nasal | 4–7 (5 ± 1, $n = 20$) | 4–6 (5 ± 1, $n = 10$) | 4–6 (5 ± 1, $n = 11$) |
| Palpebrals | 9–13 (11 ± 1, $n = 20$) | 9–14 (12 ± 1, $n = 11$) | 9–13 (11 ± 1, $n = 11$) |
| Enlarged scales between postoculars and ear | 2 (0%, $n = 20$) | 2 (44%, $n = 11$) | 2 (18%, $n = 11$) |
| | 3 (100%) | 3 (56%) | 3 (82%) |
| Enlarged lorilabials from nasal to posterior margin of orbit | 7–9 (8 ± 1, $n = 20$) | 6–9 (8 ± 1, $n = 10$) | 7–9 (8 ± 1, $n = 10$) |
| Supralabials | 6–8 (7 ± 1, $n = 20$) | 7–8 (8 ± 1, $n = 10$) | 6–8 (7 ± 1, $n = 10$) |
| Infralabials | 6–8 (7 ± 1, $n = 20$) | 7–8 (7 ± 0, $n = 11$) | 6–8 (7 ± 1, $n = 11$) |
| Gulars between first pair of infralabials | 0 (25%, $n = 20$) | 0 (0%, $n = 11$) | 0 (27%, $n = 11$) |
| | 1 (75%) | 1 (100%) | 1 (73%) |
| Chin shields | 2–6 (4 ± 1, $n = 20$) | 2–6 (5 ± 1, $n = 10$) | 2–4 (3 ± 1, $n = 10$) |
| Chin shields contacting infralabials | 2 (55%, $n = 20$) | 2 (18% $n = 10$) | 2 (36%, $n = 11$) |
| | 3 (30%) | 3(55%) | 3 (45%) |
| | 4 (15%) | 4 (27%) | 4 (18%) |
| Gulars | **25–32 (29 ± 2, $n = 20$)** | **25–33 (29 ± 3, $n = 11$)** | **24–32 (26 ± 3, $n = 11$)** |
| Ventrals | **51–61 (55 ± 3, $n = 20$)** | **48–61 (55 ± 4, $n = 11$)** | **42–61 (51 ± 5, $n = 11$)** |
| Nuchal crest scales | Males: 8–13 (10 ± 1, $n = 11$) | Males: 9–11 (10 ± 1, $n = 5$) | Males: 8–12 (10 ± 1, $n = 8$) |
| | Females: 8–11 (10 ± 1, $n = 8$) | Females: 8–10, 9 ± 1, $n = 5$) | Females: 10–11 |
| Scales spanning pectoral gap | 2–6 (4 ± 1, $n = 19$) | 1–5 (3 ± 2, $n = 11$) | 2–6 (4 ± 1, $n = 11$) |
| Dorsal crest scales | 15–17 (15 ± 1, $n = 19$) | 15–17 (16 ± 1, $n = 10$) | 14–16 (16 ± 1, $n = 10$) |
| Modified scales of dorsolateral series | 2–11 (6 ± 3, $n = 20$) | 5–7 (6 ± 1, $n = 10$) | 2–8 (5 ± 1, $n = 10$) |
| Scales around midbody | 29–41 (37 ± 3, $n = 20$) | 31–38 (35 ± 2, $n = 11$) | 31–39 (35 ± 3, $n = 11$) |
| Lamellae under Finger IV | **21–25 (23 ± 1, $n = 20$)** | **20–24 (23 ± 1, $n = 11$)** | **18–23 (21 ± 2, $n = 10$)** |
| Lamellae under Toe IV | **24–30 (26 ± 2, $n = 20$)** | **23–29 (26 ± 2, $n = 11$)** | **20–29 (24 ± 2, $n = 11$)** |
| Lamellae within span of Toe V | **8–12 (10 ± 1, $n = 19$)** | **8–11 (9 ± 1, $n = 9$)** | **6–9 (8 ± 1, $n = 9$)** |
| Bands on the tail | 8–10 (9 ± 1, $n = 17$) | 8–11 (10 ± 1, $n = 5$) | 7–9 (8 ± 1, $n = 9$) |

TABLE 3.—Results (Tukey's $Q$, $P$) of comparisons among three samples of *Lophocalotes*. NS = not significant.

| Character | Kaba | Dempo |
|---|---|---|
| Gulars | | |
| Dempo | NS | |
| Kerinci | 4.44, 0.01 | 3.39, 0.06 |
| Ventrals | | |
| Dempo | NS | |
| Kerinci | 3.82, 0.03 | 3.37, 0.06 |
| Lamellae under Finger IV | | |
| Dempo | NS | |
| Kerinci | 4.24, 0.01 | 3.71, 0.03 |
| Lamellae under Toe IV | | |
| Dempo | NS | |
| Kerinci | 4.36, 0.01 | NS |
| Toe IV lamellae within span of Toe V | | |
| Dempo | NS | |
| Kerinci | 5.47, 0.001 | 3.38, 0.06 |
| Circumorbitals | | |
| Dempo | 4.53, 0.01 | |
| Kerinci | NS | NS |
| Supralabials | | |
| Dempo | 5.24, 0.002 | |
| Kerinci | NS | NS |
| Scales spanning pectoral gap | | |
| Dempo | 3.81, 0.03 | |
| Kerinci | NS | 3.84, 0.03 |

has a relatively high frequency of two chinshields contacting the infralabials, the apparent difference is nonsignificant.

We did not find differences among populations for counts of transorbitals, loreals, palpebrals, scales around midbody, vertebral crest scales, and canthals + supraciliaries ($P > 0.10$). When we removed the effect of size by treating SVL as a covariate, we did not find relative differences in body proportions of males for the sexually dimorphic traits head length, length of the shank, length of the tail, and height of the tail at its base ($P > 0.39$). Data from both males and females, did reveal differences in body proportions for the remaining characters: head width, eye diameter, snout width, rostral width, pectoral width, length of the body, lengths of Finger IV and Toes IV and V, distance from eye to ear, and length of the tympanum ($P > 0.40$).

## Genetic Distances and Phylogeny

In preliminary analyses containing most genera of Sumatran agamids (e.g., Harvey et al. 2017b), we have consistently recovered *Lophocalotes* as sister to *Dendragama* in a clade with *Pseudocalotes*. Uncorrected pairwise genetic distances of 15.8–17.8% separate *Lophocalotes* and *Dendragama* (Table 4). Bayesian and maximum likelihood analyses

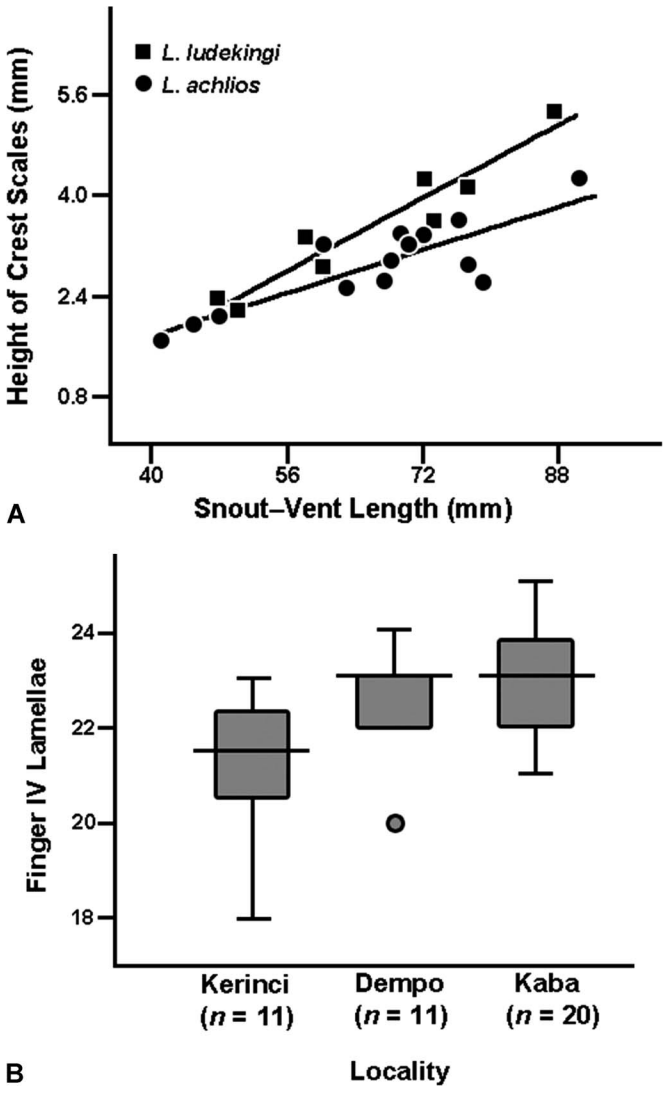


FIG. 3.—Two characters useful in distinguishing between species of *Lophocalotes*. Shaded areas of box plots represent scores between the 25th and 75th percentiles (calculated by interpolation). Circle in B represents a single near outlier.

recovered identical topologies (Fig. 4). *Lophocalotes* contains two clades, corresponding to the Kerinci population and the southern (Kaba + Dempo) samples. Uncorrected pairwise distances of 6.0–6.3% separate the southern samples from Kerinci. Nonetheless, the southern clade has weak nodal support (Fig. 4). Although distances within the Kaba and Dempo samples range from 0.0–1.7%, relatively large distances of 5.2–5.7% separate these samples from each other.

## Species Delineation

Levels of morphological divergence among the three populations mirrors that of genetic divergence: The southern populations are morphologically more similar to each other than they are to *Lophocalotes ludekingi*. Moreover, the southern populations form a monophyletic group, albeit weakly supported. Concordance of multiple morphological and molecular characters including fixed differences of nuchal crest morphology and coloration support recognition of the southern populations as a species distinct from *L. ludekingi*. Genetic distances (6.0–6.3%) between *L. ludekingi* and the southern populations are comparable to closely related species of *Dendragama* (6.0–6.4%; Harvey et al. 2017a).

Although we found morphological differences between the Dempo and Kaba populations, these differences are not fixed and are few in number. High, genetic distances (5.2–5.7%) between these two populations are comparable to distances among allopatric populations of some other montane agamids such as *Pseudocalotes tympanistriga* (Harvey et al. 2017a), but they do not exceed distances among species pairs in related genera as cited above. Without more compelling evidence, we consider the Dempo and Kaba populations to be conspecific. However, we do not include the Dempo sample in the type series of the new species. We accept the conclusions of Hallermann et al. (2004) that the Kerinci population is *Lophocalotes ludekingi,* and we describe the species constituted by the southern populations as follows.

## Description

### *Lophocalotes* ***achlios*** sp. nov.

**Holotype.**—An adult male (MZB 14038, field tag ENS 18170; Figs. 1, 2A,B) collected 16 July 2015 by M.B. Harvey, E. Wostl, G.C. Sarker, and P. Thammachoti along the main trail up Gunung Kaba, Kabupaten Rejang Lebong, Provinsi Bengkulu, Sumatera, Indonesia, 3.50757°S, 102.62927°E, 1818 m above sea level (a.s.l.).

**Paratypes (n = 20).**—Eleven males (MZB 14030, 14032, 14033, 14037–14039, UTA 63730, 63733, 63735–63737) and eight females (MZB 14031, 14034–14036, UTA 63729, 63731, 63732, 63734) collected on 16 July 2015 by M.B. Harvey, E. Wostl, G.C. Sarker, and P. Thammachoti along the main trail up Gunung Kaba, 3.50026–3.50757°S, 102.62927–102.63557°E, 1567–1818 m a.s.l.; and one male (UTA 63740) collected by E.N. Smith, E. Wostl, G.C. Sarker, and G. Pradana on 22 July 2015 from a trail up Gunung Kambing above the police academy near the road to Gunung Kaba, 3.39649°S, 102.63599°E, 1636 m a.s.l., Kabupaten Rejang Lebong, Provinsi Bengkulu, Sumatera, Indonesia.

**Referred specimens (n = 10).**—One male (UTA 63739) and three females (MZB 14040, and UTA 63728 and 63738)

TABLE 4.—Uncorrected pairwise genetic distances for ND4 sequences between specimens of *Lophocalotes* and *Dendragama boulengeri*.

| | *Lophocalotes ludekingi* (Kerinci, Tujuh; n = 4) | *L. achlios* (Kaba, n = 2) | *L. achlios* (Dempo, Patah, n = 2) | *D. boulengeri* (Marapi, n = 1) |
|---|---|---|---|---|
| *Lophocalotes ludekingi* (Kerinci, Tujuh) | 0.0–0.6% | 6.3% | 6.0% | 15.8–16.3% |
| *L. achlios* (Kaba, Kambing) | | 0.0% | 5.2–5.7% | 17.2% |
| *L. achlios* (Dempo, Patah) | | | 1.7% | 17.8% |
| *Dendragama boulengeri* (Marapi) | | | | — |

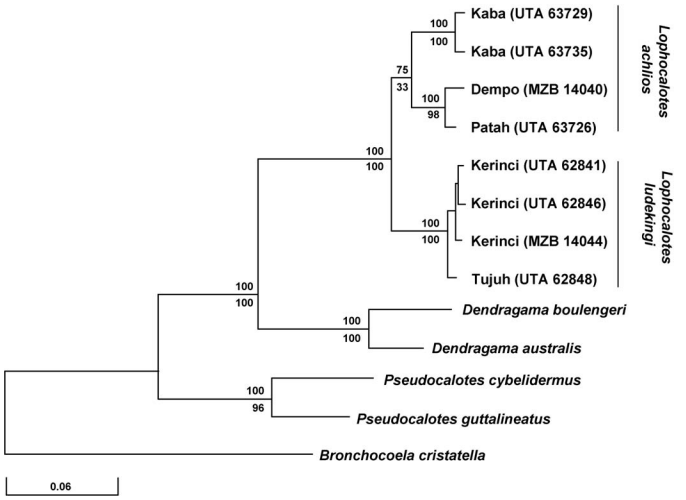


FIG. 4.—Fifty percent majority rule consensus phylogram of *Lophocalotes*. Scale bar (substitutions per site) and branch lengths are derived from the Bayesian tree. Percent posterior probabilities appear above branches and bootstrap values appear below branches.

collected 8–15 July 2015 by M.B. Harvey, E. Wostl, U. Smart, P. Thammachoti, G. Pradana, G.C. Sarker, and F. Alhadi along a trail above Kampung Empat, Gunung Dempo, 40411–4.0407°S, 103.13706–103.14823°E, 1807–2526 m a.s.l.; one male (UTA 62888) collected on 3 June 1996 by M.B. Harvey and E.N. Smith on the southeast side of Gunung Dempo, 04°03′03"S, 103°08′40"E, 1690 m a.s.l.; three males (MZB 14028, 14029, UTA 63727) and two females (MZB 14027, UTA 63726) collected on 12 July 2015 by E. Wostl and G.C. Sarker along a trail up Gunung Patah 4.2098–4.2287°S, 103.41467–103.4365°E, 1626–2050 m a.s.l., Kabupaten Lahat, Provinsi Sumatera Selatan, Sumatera, Indonesia.

**Diagnosis.**—A species of *Lophocalotes* differing from the *L. ludekingi* in having more gulars, ventrals, and subdigital lamellae; in having males with a lower nuchal crest not supported by an arched flap of skin and white gular markings; and in having females with cream buccal epithelia.

**Description of type series.**—Characteristics of the holotype appear in brackets after other male specimens. Males reaching 247 mm (SVL 90 mm) [247, 90] and females reaching 183 mm in length; smallest juveniles in our sample 71 mm (SVL 26 mm) total length; SVL 34.0–38.4% (36.4 ± 1.1%, $n = 12$) [36.4%] and tail 61.6–66.0% (63.6 ± 1.1%, $n = 12$) [63.6%] of total length in males; SVL 36.1–39.4% (37.8 ± 1.1%, $n = 8$) and tail 60.6–63.9% (62.2 ± 1.1%, $n = 8$) of total length in females; tail 1.604–1.940 times (1.750 ± 0.087, $n = 12$) [1.744 times] as long as SVL in males and 1.535–1.773 (1.650 ± 0.074, $n = 8$) as long as SVL in females; distance from axilla to groin accounting for 37.8–49.0% (45.5 ± 3.1%, $n = 19$) [45.5%] of SVL; head 64.4–82.9% (72.1 ± 5.0%, $n = 11$) [82.9%] as wide as long in males and 69.2–74.2% (71.5 ± 1.6%, $n = 8$) as wide as long in females, accounting for 23.3–27.2% (25.4 ± 1.2%, $n = 11$) [24.9%] of SVL in males and 22.5–26.3% (24.8 ± 1.1%, $n = 8$) of SVL in females; snout subacuminate in dorsal view and in profile, sloping upward at about 30° to horizontal (Fig. 1); dorsal head scales weakly imbricate, keeled; rostral visible from above, 63.0–81.4% (73.5 ± 5.8%, $n = 19$) [74.9%] as wide as internarial distance, its height 19.5–43.2% (28.7 ± 5.7%, $n = 19$) [27.0%] of its width, broadly contacting first supralabials and four (40%, $n = 20$) or five (50%) small postrostrals [five]; postrostral series contacting nasal (100%, $n = 20$); noticeably enlarged scales arranged as inverted Y or V on snout; each "arm" of Y usually consisting of one large scale separated from base by one small scale, reaching anteromedial border of orbit and with keel directed posterolaterally; arms of Y noticeably raised and flanking slightly depressed prefrontal region; scales of frontal region about as large as medial supraoculars, much smaller than scales of circumorbital series; parietal and occipital regions somewhat depressed, bound laterally and posteriorly by rounded ridge along somewhat swollen skin covering supratemporal region and skin just in front of nuchal crest; interparietal usually present (85%, $n = 20$) [present], elongate and roughly diamond-shaped, separated from circumorbital series by oblique row of few enlarged, heavily keeled scales each as large or larger than circumorbitals; parietal eye usually evident as depressed circular area usually in center of keel or at a bifurcation of keel, sometimes more pale than surrounding surface of scale.

One (15%, $n = 20$), two (75%), or three (10%) [two] supranasal scales separating postrostral series from first canthal; circumorbital scales 7–11 (9 ± 1, $n = 20$) [10], distinctly enlarged, roughly pentagonal to octagonal, extending between canthal series and postciliary scale; transorbitals 12–15 (13 ± 1, $n = 20$) [13]; canthals four (20%, $n = 20$), five (50%), or six (30%) [five]; supraciliaries five (20%, $n = 20$), six (60%), or seven (20%) [five]; combined count of canthals and supraciliaries 10–13 (11 ± 1, $n = 20$); direction of imbrication changing along supraciliary series: posterior edges of anterior supraciliaries imbricating onto medial side of next posterior scale, anterior edges of posterior one or two supraciliaries imbricating onto medial side of next anterior scale, and one or two supraciliaries in center of eye not imbricating; supraciliary notch distinct; 1–3 [2] small scales separating last supraciliary from postciliary scale; postciliary scale prominent, subpyramidal to pyramidal, single, positioned at dorso-posterior corner of orbit; temporal modified scale and one supratemporal immediately in front of it heavily keeled, remaining scales of temporal region feebly keeled, angulate, weakly imbricating posteroventrally; temporal modified scale resembling other supratemporals but more heavily keeled and with low but distinct, projecting apex; posttemporal modified scale enlarged, single, pyramidal to spinose, contacting temporal modified scale (20%, $n = 20$) or separated from it by single small scale of neck (80%) [separated].

Nasal large, oval to trapezoidal, its dorsal border contributing to canthus; nasal contacting supralabial 1 (85%, $n = 20$) or both 1 and 2 (15%) [1 only]; nostril large, oval, directed laterally, its upper margin reaching canthus; scales of loreal region smooth or feebly keeled, 4–7 (5 ± 1, $n = 20$) [6] scales in vertical row between last canthal and supralabials, 4–7 (5 ± 1, $n = 20$) [6] scales in horizontal row from anterior border of orbit to nasal; orbit 32.9–40.9% (35.6 ± 2.2%, $n = 11$) [32.9%] of head length in males, 33.2–38.6% (36.8 ± 2.0%, $n = 8$) of head length in female; palpebrals granular; second row of palpebrals above eye containing 9–13 (11 ± 1, $n = 20$) [13] scales between ocular angles, central 1–4 of these largest and more heavily keeled;

large subocular scale row broadly contacting supralabials and not separated from supralabials by row of small lorilabials (100%, $n = 20$); 7–9 ($8 \pm 1$, $n = 20$) [9] lorilabials from nasal to posterior border of orbit; large distinctive oval to rectangular lorilabial positioned above last supralabial and short, elongate scale bordering rictal fold, separated from other enlarged lorilabials by vertical row of small scales; horizontal row of three (100%, $n = 20$) enlarged, angulate scales between orbit and anterior margin of auditory meatus; tympanum large, thin and translucent, 40.6–65.0% ($52.3 \pm 6.3\%$, $n = 19$) [65.0%] of diameter of orbit, 16.6–21.4% ($19.1 \pm 1.6\%$, $n = 11$) [21.4%] of head length in males and 16.8–20.3% ($18.4 \pm 1.2\%$, $n = 8$) of head length in females; distance from border of auditory meatus to orbit 21.1–30.5% ($24.8 \pm 3.0\%$, $n = 11$) of head length in males, 20.5–26.6% ($24.4 \pm 2.0\%$, $n = 8$) of head length in females; scales surrounding meatus small and angulate, resembling adjacent scales; posttympanic modified scale positioned slightly below dorsolateral crest, more heavily keeled than adjacent scales and enlarged to somewhat subpyramidal, smaller than modified posttemporal scale; posttympanic modified scale surrounded by smaller scales (60%, $n = 20$), abutting one additional enlarged heavily keeled scale (30%), or in short oblique row of three enlarged, heavily keeled scales (10%) (surrounded by smaller scales).

Supralabials smooth, 6–8 ($7 \pm 1$, $n = 20$) [7]; rictal fold short, bordered dorsally and ventrally by one or two elongate scales behind labial series; infralabials smooth, 6–8 ($7 \pm 1$, $n = 20$) [7]; chin shields 2–6 ($4 \pm 1$, $n = 20$) [4], first two (55%, $n = 20$), three (30%), or four (15%) [two] contacting infralabials (thereafter, sublabial scales separating enlarged chin shields from infralabials); first pair of chin shields in medial contact (25%, $n = 20$) or separated medially by one (75%) gular (separated by one gular); gulars smooth to feebly keeled, 25–32 ($29 \pm 2$, $n = 20$) [28] from mental (or point of medial contact between first pair of chin shields) to preaxial margin of arm, arrayed as 23–31 ($27 \pm 2$, $n = 11$) [27] interrictal scales between last right and left infralabials; gular pouch weakly developed, longitudinal; transverse gular fold weak; gulars relatively small in center of pouch, laterally increasing in size threefold; sublabial tuberculate scales and postrictal modified scale absent.

Nuchal crest prominent, consisting of 5–9 ($7 \pm 1$, $n = 19$) long lanceolate scales separated from one another by paravertebrals or much smaller projecting scales; first lanceolate nuchal crest scale separated from occiput by 2–4 small triangular scales mostly contacting one another; total nuchal crest scales 8–13 ($10 \pm 1$, $n = 11$) [11] in males and 8–11 ($10 \pm 1$, $n = 8$) scales in females; longest nuchal crest scales 15.0–21.0% ($17.5 \pm 2.0$, $n = 10$) [19.1%] as long as head and 72.0–109.1% ($90.9 \pm 11.1\%$, $n = 10$) [89.4%] as long as tympanum in males, 11.7–17.8% ($14.1 \pm 2.0\%$, $n = 8$) as long as head and 67.5–91.1% ($77.0 \pm 8.9\%$, $n = 8$) as long as tympanum in females; dorsal crest prominent, serrate, extending onto base of tail in both sexes, though somewhat less raised posteriorly in females; nuchal crest consisting of transversely narrow scales with heavy keels and long, projecting tips; 15–17 ($15 \pm 1$, $n = 19$) [16] enlarged projecting scales in dorsal crest to posterior border of thigh; single pairs of paravertebrals or small low vertebrals mostly separating large dorsal crest scales except anteriorly where first 2–4 projecting scales contact one another and directly above the leg where 2–6 projecting scales contact one another; largest scales of dorsal crest 76.0–101.4% ($85.6 \pm 9.4\%$, $n = 10$) [82.7%] as long as largest nuchal crest scales in males and 87.7–106.7% ($95.6 \pm 6.7\%$, $n = 8$) as long as largest nuchal crest scales in females; scales of dorsal crest separated from nuchal crest by pectoral gap of 2–6 ($4 \pm 1$, $n = 19$) [4] small dorsals; paravertebral series same size as adjacent dorsals.

Dorsals much larger than ventrals; on neck, posttympanic series in line with enlarged scales between orbit and tympanum, consisting of one (58%, $n = 19$), two (21%) or three (21%) [two] slightly enlarged heavily keeled scales with their keels directed at slightly different angle than adjacent scales and situated about halfway between scapula and tympanum; additional enlarged and more heavily keeled scale positioned about halfway between lower border of tympanum and scapula; above posttympanic series, dorsals pointing upward and backward; scales of posttympanic series and dorsals below them pointing backward or downward and backward without reorientation at antehumeral fold; at midbody, upper 5–8 ($7 \pm 1$, $n = 20$) [7] rows of dorsals pointing upward and backward, scale row below them pointing backward, and lower scales pointing backward and downward; in most specimens (75%, $n = 20$), dorsolateral series including two widely separated, enlarged, heavily keeled (often even projecting), white scales [holotype has this pattern]; in these specimens, first modified scale of dorsolateral series positioned one-third of distance between limbs and second white scale positioned two-thirds of distance between limbs; remaining 25% of specimens with three white scales in dorsolateral series, first positioned below anterior terminus of dorsal crest; other scales of dorsolateral series green, less heavily keeled, and variably present, usually forming closely spaced or continuous series between last white scale and level of thigh; including both white and green scales, dorsolateral series containing 2–11 ($6 \pm 3$, $n = 20$) [5] heavily keeled scales; first scale of dorsolateral series separated from dorsal crest by three or four [three] scales, last separated from dorsal crest by 2–4 [2] scales; scales of dorsolateral crest contacting one another or separated by 1–8 scales (white scales always widely separated, whereas green scales between last white scale and thigh usually in contact with one another); scales of lower flanks usually (80%, $n = 20$) homogeneous, four specimens (20%) with several larger heavily keeled scales interspersed among much smaller, feebly-keeled scales below dorsolateral series (scales on lower flanks of holotype homogeneous); scales around midbody 29–41 ($37 \pm 3$, $n = 20$) [35]; ventrals keeled, small with sharp transition to much larger scales on flanks, 51–61 ($55 \pm 3$, $n = 20$) [55] from preaxial edge of arm to vent.

Base of tail modified in males, higher and thicker than rest of tail; width of base of tail 71.5–93.7% ($83.8 \pm 7.2\%$, $n = 10$) [86.6%] of height of tail in males, 81.6–107.8% ($89.6 \pm 8.8\%$, $n = 8$) of height of tail in females; dorsal crest scales on base of tail of males somewhat rugose, wider and larger than crest scale above limbs (females might also have somewhat wider scales at the base of their tails, but the difference between these and those above the limbs is not as obvious as in males); differentiated dorsal crest not extending beyond proximal one-fourth of tail; throughout length of tail, subcaudals about same size as scales on sides of tail.

Scales of brachium, antebrachium, thigh, and shank imbricate, keeled; one or two noticeably enlarged and more heavily keeled scales positioned along postaxial border of antebrachium within white bands crossing arm; distal modified antebrachial scale separated from wrist by three scales and by one scale from proximal modified scale when present [holotype with 1/1 noticeably enlarged antebrachial scale; two keels on scale of right arm]; keels of modified antebrachials oriented more postaxially than adjacent scales; 2–4 (3 ± 1, $n = 19$) [2] similar enlarged scales with pointed blade-like keels arrayed along postaxial margin of dorsal thigh; modified scales on thigh with keels directed more postaxially than adjacent scales and always consisting of one particularly large scale with its keel oriented distally and one smaller scale with its keel oriented proximally; 2–4 [4/3] abruptly enlarged and more heavily keeled scales crossing dorsal side of shank in third row of scales below knee; palmar and plantar scales, imbricating distally, smooth, devoid of mucrons; subdigital lamellae entire; few distal lamellae bicarinate with low, indistinct keels; lamellae 21–25 (23 ± 1, $n = 20$) [22] under Finger IV; Finger III 92.3–106.8% (100.1 ± 3.3, $n = 11$) [106.8%] as long as Finger IV; Finger IV 64.4–75.7% (70.6 ± 3.0, $n = 18$) [64.4%] as long as Toe I; lamellae 24–30 (26 ± 2, $n = 20$) [27] under Toe IV; single subdigital and single supradigital ungual lamellae contacting one another on all fingers and toes; ungual lamellae much longer than other subdigital lamellae; in relative length, Finger III = IV > II > V > I and Toe IV > III > V > II > I; Toe V 70.4–79.3 (75.9 ± 2.4, $n = 18$) [71.9%] as long as Toe IV; when adpressed, 8–12 (10 ± 1, $n = 19$) [10] lamellae under Toe IV within span of fifth toe; leg short in length relative to other draconines; shank 15.3–19.6% (17.3 ± 1.1%, $n = 19$) [18.3%] of SVL.

Scale organs lenticular, single and positioned subterminally, usually just below mucrons on body, more numerous and also concentrated on keels on head; bristled sense organs (sensu Ananjeva et al. 1991) present, position, number and distribution not assessed; callous glands absent; femoral and precloacal pores absent.

Coloration (based on photos of holotype and MZB 14039 in life and photos of 16 paratypes taken shortly after they were euthanized): dorsal scales of head green with black sutures or brown; when visible, brown scales of dorsal head forming irregular bands and blotches; first row of palpebrals from eye yellow and white; remaining palpebrals green with yellow lines radiating out from eye; posttemporal and posttympanic modified scales immaculate green or yellow, contrasting with brown scales below them; diffuse brown and green postocular patch bound dorsally by keels of enlarged orbito-tympanic scales and ventrally by lorilabial series, tympanum brown; patch of white scales absent from below and behind tympanum in most specimens (small patch of white scales in two male specimens [20%, $n = 10$ males], absent in all females [$n = 8$]: covering parts of four scales in holotype and parts of three scales in MZB 14033); distinct white stripe below eye (entirely covering lorilabial scales, but not extending onto supralabials); labials green with some diffuse white blotching or banded green and brown; gulars green with prominent white to pale bluish white blotches occupying patches of 1–4 scales, but sometimes forming oblique lines 1–2 scales wide and extending to midgular region; in some specimens, white to pale bluish coloration extending onto anterior chest and forming broad patch (e.g., MZB 14033) or transverse band (e.g., holotype).

Neck mostly green with irregular brown edging of some scales; one roughly diamond-shaped brown blotch with darker edging positioned vertebrally and overlapping posterior few scales of nuchal crest; nuchal crest same color as adjacent paravertebrals with some mostly green and some mostly brown scales; distinct pinkish white saddle straddling most of pectoral gap and anterior end of first dorsal crest scale, extending laterally to cover small scales of dorsolateral crest; sharp brown line extending from dorsoposterior edge of tympanum to back of head where it fuses with wider somewhat bifurcate patch of brown scales that curve around anterior border of arm across antehumeral fold.

Body mostly green with three (100%, $n = 17$) [three] diamond-shaped vertebral blotches; blotches often barely visible in males, in females prominent, brown, edged in dark brown or black, with their apexes reaching dorsolateral crest; two largest and most heavily keeled scales of dorsolateral series white in most specimens (more posterior one yellow in holotype); when present, heavily keeled scale just behind scapula also white; if present, additional heavily keeled scales of dorsolateral series same color as adjacent scales; lower flanks and ventrolateral region green with numerous staggered white scales sometimes forming broken bands; midventral region nearly immaculate green in males, white or dull tan in females.

Eight to ten (9 ± 1, $n = 17$) [9] bands on tail; tail green and brown proximally becoming brown and darker brown distally; each caudal band with darker brown edging and each caudal interspace with paler edging; first caudal band more of a diamond-shaped blotch resembling those on body; length of bands variable, mostly longer than interspaces, incomplete ventrally or complete ventrally but somewhat constricted so that interspaces longer; proximal subcaudals resembling body in being immaculate green.

Limbs mostly green with evenly spaced white or yellow bands, each band one scale row wide and sometimes incomplete or represented only by white or yellow keels on otherwise mostly green scales; three evenly spaced bands crossing brachium; two bands on antebrachium including modified scales positioned along postaxial margin and one narrow, incomplete band at wrist; three bands crossing thigh, middle one including large modified scale on postaxial margin; two bands crossing shank, more proximal band covering transverse row of enlarged, heavily keeled scales; digits banded dark brown or black with green or yellow interspaces; dorsal ungual scale white or yellow and contrasting with rest of digit; soles of hands and feet cream to charcoal appearing to darken with increasing SVL.

Iris bronze with complete light gold ciliary ring; buccal epithelium bright yellow-orange in males; parietal peritoneum black; visceral peritoneum unpigmented.

**Measurements of holotype (in mm).**—SVL 90, length of tail 157, length of body 41.0, pectoral width 14.8, length of head from occiput to rostral 22.4, length of head from anterior border of auditory meatus to rostral 23.4, width of head 18.6, length of orbit 7.4, distance from orbit to tympanum 6.8, length of tympanum 4.8, height of largest scale of nuchal crest 4.3, height of largest scale of dorsal crest 3.6, width of snout 5.0, width of rostral 3.7, height of rostral

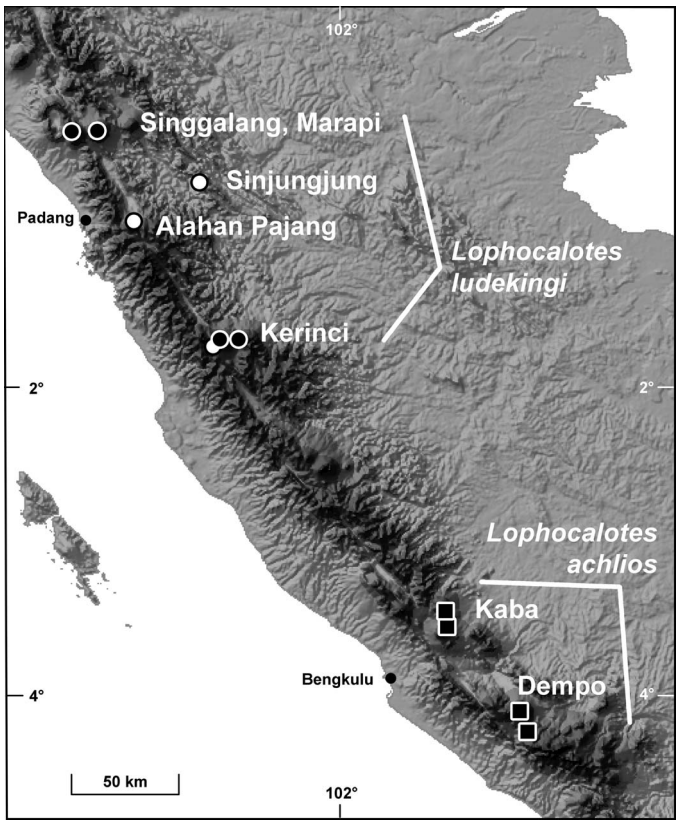


FIG. 5.—Central Sumatra showing known distribution of *Lophocalotes*. Open symbols represent specimens reported by Hallermann et al. (2004), but not examined by us.

1.0, length of shank 16.4, length of Finger IV 10.3, length of Finger III 11.0, length of Toe IV 16.0, length of Toe V 11.5.

**Variation among referred specimens.**—In general, specimens from Gunung Dempo and Gunung Patah were more heavily mottled in brown than specimens of the type series. The curved marking on the neck does not bifurcate as in most specimens from Kaba and appears wider. The swollen section of the tail of MZB 14042 was almost entirely white dorsally and ventrally except for brown keels on each scale. A photo of this specimen with its gular pouch extended reveals aquamarine-colored skin between the gular scales.

We report most noteworthy meristic variation in Table 2. In addition to these characters, one specimen from Patah and one from Dempo (18%, $n = 11$) have single small scales intercalated between the nasal and postrostral series, whereas one postrostral separates the nasal and rostral in the remaining specimens. Seventy percent of specimens ($n = 10$) from Dempo and Patah have a discrete interparietal. Whereas all specimens of the type series have three enlarged scales between the external auditory meatus and orbit, 45% ($n = 11$) of the specimens from Dempo and Patah have only two scales and the remaining specimens (55%) have three.

**Etymology and standard English name.**—The specific epithet *achlios* is a feminine noun in apposition derived by affixing the Greek suffix *–ios* meaning "pertaining to" or "of" to *achlys*, meaning mist. The new name refers to the misty cloud forests where *Lophocalotes achlios* occurs. We propose the standard English name "White-throated Crested Dragons" for this species in reference to the pattern of white and green on its gular scales.

**Distribution and ecology.**—*Lophocalotes achlios* occurs on four volcanoes in the southern Bukit Barisan Range of Sumatra (Fig. 5). Ninety straight-line kilometers separate the type locality (Gunung Kaba) in southern Bengkulu Province from Gunung Dempo in northern Sumatera Selatan, and an additional 33 straight-line kilometers separate Dempo from Patah, further to the south. We collected all of the *L. achlios* in closed-canopy, upper montane rainforest while the lizards were sleeping 1.0–5.5 m aboveground in understory vegetation between 1830 and 0057 h. On Dempo and Patah, *Lophocalotes achlios* occurs in microsympatry with *Dendragma australis*. *Pseudocalotes cybelidermus* and *P. guttalineatus* occur on all four volcanoes; however, these species occur along the forest edge on Dempo and Patah, whereas *L. achlios* and *D. australis* appear to be restricted to the forest interior. On Gunung Kaba, we found the two species of *Pseudocalotes* to be numerous in low vegetation, but also largely restricted to areas with a mostly open canopy along the trail. *Lophocalotes achlios* occurred at lower densities than *Pseudocalotes* on Kaba, and we found most specimens just inside the forest edging the trail. These four agamids grow to about the same size as adults with SVL < 100 mm. Of the four, *Lophocalotes achlios* is the only species with a prehensile tail. It is more slow-moving and undergoes somewhat less pronounced color change than the other three species.

*Lophocalotes achlios* may best be described as a generalist predator (niche breadth = 5.64). We recorded 12 categories of food in the diets of *L. achlios* (Table 5), and this species primarily consumes ants, millipedes, and insect larva (mainly lepidopteran). Although these three food categories comprise 68% of the items in our sample, millipedes and larvae account for substantially more of the volume and, therefore, are the most important prey items.

Males and females had similar niche breadths, and our contingency table did not indicate differences between the sexes for diet ($P_{11} = 0.39$). Although nonsignificant, females nonetheless ingested more isopods than males (Table 5), and isopods were the second most numerous food item in the diets of females after millipedes.

From the intestine, we recovered 100 specimens of a previously undescribed nematode (now named *Spinicauda sumatrana* Bursey et al. 2017) and two specimens of an unidentified trematode (tentatively referred to *Paradistomoidella* Brooks and Palmier 1981; C.R. Bursey and S.R. Goldberg, personal observations). The paratypes carried a load of 0–12 ($4 \pm 4$, $n = 28$) nematodes with a mean intensity of infection (average number of parasites in infected hosts) of 5. In our sample, parasite load increases with SVL (Pearson's $r = 0.53$, permutation $P_{\text{uncorrelated}} = 0.006$). The smallest specimen infected by nematodes had a SVL of 48 mm; four small juveniles (26–45 mm SVL) and two adults (62 and 68 mm) were not infected. Excluding the four uninfected juveniles from the comparison, we did not find a sexual difference in parasite load ($t_{12,12} = 0.30$, $P = 0.77$).

In *Lophocalotes achlios*, *Spinicauda sumatrana* has an aggregated population structure as indicated by the relatively high coefficient of dispersion of 3.78 and relatively close fit to a negative binomial distribution ($k = 1.967$, Fisher's exact

TABLE 5.—Diet of *Lophocalotes achlios*. For comparison, counts and percentages of total food items for males and females are reported separately. The last column (Frequency) reports number of lizard specimens containing the food category.

| | Males ($n = 14$) | | Females ($n = 14$) | | Both sexes ($n = 28$) | | | | |
|---|---|---|---|---|---|---|---|---|---|
| | Prey count | Percent | Prey count | Percent | Prey count | Percent | Volume ($mm^2$) | Percent volume | Frequency |
| Insect larva | 12 | 23.50 | 8 | 16.00 | 20 | 19.8 | 119,686.50 | 60.80 | 12 |
| Millipedes | 11 | 21.60 | 10 | 20.00 | 21 | 20.80 | 59,591.30 | 30.30 | 12 |
| Hymenoptera (ants) | 14 | 27.50 | 13 | 26.00 | 27 | 27.00 | 2,288.21 | 1.16 | 12 |
| Snails | 2 | 3.92 | 3 | 6.00 | 5 | 5.00 | 664.14 | 0.34 | 4 |
| Spiders | 1 | 1.96 | 2 | 4.00 | 3 | 3.00 | 1.80 | 0.00 | 3 |
| Isopods | 3 | 5.88 | 9 | 18.00 | 12 | 11.90 | 15,844.40 | 8.05 | 5 |
| Coleoptera | 2 | 3.92 | 4 | 8.00 | 6 | 5.94 | 666.11 | 0.34 | 6 |
| Hymenoptera (bees) | 2 | 3.92 | 0 | 0 | 2 | 2.00 | 0 | 0 | 2 |
| Orthoptera | 1 | 1.96 | 0 | 0 | 1 | 1.00 | 0 | 0 | 1 |
| Collembola | 2 | 3.92 | 0 | 0 | 2 | 2.00 | 24.41 | 0.12 | 2 |
| Diptera | 1 | 1.96 | 0 | 0 | 1 | 1.00 | 0 | 0 | 1 |
| Phthiraptera | 0 | 0 | 1 | 2.00 | 1 | 1.00 | 3.70 | 0.00 | 1 |
| Total | 51 | 100.00 | 50 | 100.00 | 101 | 100.00 | 198,770.57 | 101.00 | |
| Niche breadth | 5.31 | | 5.64 | | 5.64 | | | | |

test $P = 0.94$; Fig. 6). Nonetheless, we could not reject the alternative hypothesis of random assembly of nematode communities (Poisson model; Fisher's exact test $P = 0.20$), likely because of small sample sizes.

In our sample, two specimens of *Lophocalotes achlios*, 44 and 49 mm SVL, had not reached reproductive condition. The remaining 11 females, 58–71 mm SVL, all contained oviductal eggs, large yolky ovarian follicles, or both. The gravid females (73% of 11 sexually mature specimens) contained two (38%, $n = 8$), three (13%), four (38%), or six (13%) oviductal eggs 12.1–17.5 mm (14.3 ± 1.6 mm, $n = 8$) long and 5.9–7.5 mm (6.6 ± 0.5 mm, $n = 8$) wide, volume 219.5–508.1 $mm^3$ (331.2 ± 86.2 $mm^3$, $n = 8$). Each ovary of mature females contained 5–9 (7 ± 2, $n = 8$) developing follicles, the largest 2.1–6.0 mm (4.2 ± 1 mm, $n = 11$) in diameter. The largest follicles were usually yolky, even in specimens with oviductal eggs, indicating that *L. achlios* lays multiple clutches each year. The two immature females each had four developing follicles in their ovaries, 1.1–1.2 mm in diameter. Thus, female *L. achlios* reach sexual maturity between 50–57 mm SVL, have a clutch size of 2–6 eggs, and likely produce multiple clutches per year. Number of ovarian follicles increases with SVL ($r = 0.64$, $t_{13} = 2.35$, $P = 0.05$) as described by the regression line: number of follicles = 0.13 * SVL – 1.79. We did not find a correlation between SVL and clutch size ($t_{12} = 0.22$, $P = 0.84$); however, the 12 specimens containing oviductal eggs fell within a relatively narrow range of SVLs (65–71 mm). In contrast, our follicular counts came from specimens ranging from 44 to 71 mm SVL.

*Lophocalotes achlios* evidently delays oviposition until its oviductal eggs have developed to a large size. Even with the digestive tract removed, we noted the surprisingly small coelomic space not occupied by oviductal and advanced ovarian eggs. To accommodate eggs, the right gonad of both sexes is positioned slightly anterior to the left in all specimens. When advanced yolky ovarian eggs are present, the advanced egg of the right ovary often abuts the anterior end of the left advanced egg. In specimens with single eggs in each oviduct, the right egg was always positioned anterior to the left egg. This positioning appears to accommodate the stomach, which typically abuts the anterior end of the left oviductal egg.

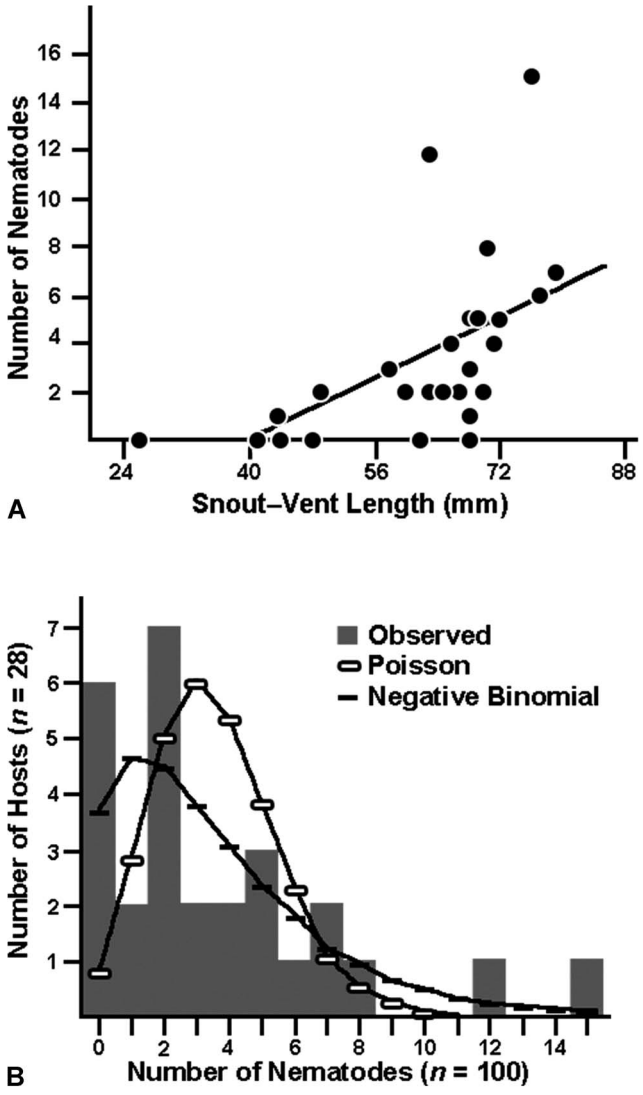


FIG. 6.—Parasite load of the nematode *Spinicauda sumatrana* in *Lophocalotes achlios*. (A) Correlation of parasite load and snout–vent length, (B) observed parasite load compared to loads predicted under aggregated (negative binomial) and random (Poisson) models of infection rates.

Among the male specimens, five specimens 26–60 mm SVL had straight vasa efferentia and did not appear to have reached sexual maturity. The remaining specimens (62–90 mm SVL) had coiled vasa efferentia and appeared to be sexually mature. Thus, male *Lophocalotes achlios* reaches sexual maturity at a longer SVL than females, between 60 and 62 mm.

Male *Lophocalotes achlios* grow to a substantially larger size (maximum SVL 90 mm, total length 247 mm) than females (maximum SVL 71 mm, total length 193 mm). Our sample of 29 specimens contains all size classes, and 5 of the male specimens (29%, $n = 17$ males) are longer than the longest female. At its base, the tail is relatively higher in adult male *L. achlios* than in adult females; however, this sexually dimorphic trait does not appear until lizards exceed 50 mm SVL. Male *L. achlios* have more nuchal crest scales than females (Welch's $t_{15,13} = 2.18$, $P = 0.04$; Fig. 7). When we removed the effect of size by treating SVL as a covariate, males have longer tails ($F_{1,26} = 11.44$, $P = 0.002$), shanks ($F_{1,25} = 6.49$, $P = 0.02$), and nuchal crest scales ($F_{1,24} = 18.74$, $P < 0.001$) than females. Males have relatively longer heads whether head length is measured from the tympanum ($F_{1,24} = 7.31$, $P = 0.01$) or from the occiput to the tip of the snout ($F_{1,25} = 4.36$, $P = 0.05$). We did not find sexual dimorphism in relative head width, pectoral width, body length or in counts of ventrals or dorsal crest scales. Although we did not find head width to be dimorphic, our conclusions would likely change if we had taken the measurement behind and below the ear instead of at the rictus: adult males develop noticeably hypertrophied jaw muscles, visible below the ear as prominent swellings.

Although sexually dimorphic, sexual dichromatism is somewhat limited in this species. Usually, males have green bellies and indistinct dorsal bands, whereas females have white bellies and distinct brown diamond-shaped dorsal bands (Fig. 2F). An exception to this pattern is UTA 63740, a 67-mm-SVL male with a white venter. Presence of a patch of white scales below and behind the ear may be a dichromatic character in lizards from Gunung Dempo and Gunung Patah: All five males from these localities had a patch covering 4–9 scales, whereas four females lacked a patch and a single female had a patch covering parts of three scales. Lacking photos of females with open mouths from the type locality, we do not know if they share the cream buccal epithelia of females from Gunung Dempo. Males at both localities have yellow–orange buccal epithelia.

We have limited data on color change in the type series, because we only have photos in life of two specimens, the holotype and a small juvenile male. Throughout a somewhat lengthy photo session, the holotype did not change color. Immediately after being euthanized, however, the specimen darkened overall and banding became more pronounced: on dorsal surfaces of the head, broken transverse brown bands about one scale thick crossed the internarial region, just behind the nasal, and at mid-canthus. The depressed prefrontal region was covered in a large diffuse brown blotch, and the circumorbitals were mostly brown. These same scales were green with black edging in life. The large scales below the ear darkened almost to black and white ventral scales turned pale blue. Labials and scales on the face also darkened and cream spots appeared. More pale bands appeared on the limbs: immediately after death, the

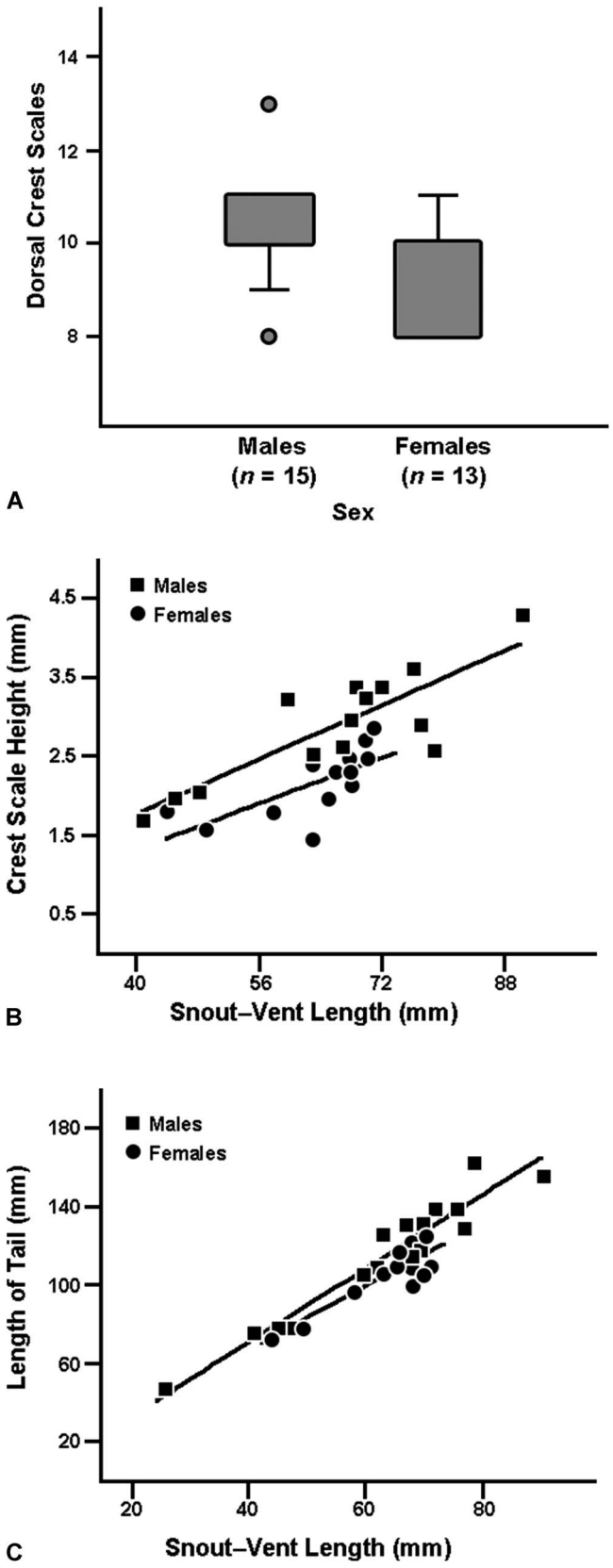


FIG. 7.—Sexual dimorphism in three characters of *Lophocalotes achlios*. Shaded areas of box plots include scores between the 25th and 75th percentiles (calculated using interpolation). Circles in A are single near outliers.

specimen had three rather than two bands on the brachium, four rather than three bands on the antebrachium, four rather than two bands on the thigh, and two rather than one band on the shank. In contrast, an adult male from Gunung Dempo (MZB 14028) was heavily mottled with brown when alive, but changed to mostly green after being euthanized.

## Discussion

Two diagnostic characters of *Lophocalotes* deserve additional comment. At least since the publication of Boulenger's (1885) Catalogue of Lizards in the British Museum, researchers have known about the diagnostic smooth subdigital lamellae of *Lophocalotes*. Lack of subdigital keels immediately distinguishes this genus from all other Southeast Asian agamids. What is less well known is that the keels have also been lost across scales of the palmar and plantar surfaces, and vestigial keels remain on the distal phalanges.

Previous descriptions of *Lophocalotes ludekingi* (De Rooij 1915; Manthey and Grossmann 1997; Hallermann et al. 2004) did not mention that this species has a prehensile tail. This characteristic of both *L. ludekingi* and *L. achlios* distinguishes these species from most draconines, including their close relatives *Dendragama* and *Pseudocalotes*. Notably, *Lophocalotes* shares this trait with another cryptic arboreal Sumatran species: *Pseudocophotis sumatrana* (Hubrecht 1879; see also Manthey and Denzer 2000; Ananjeva et al. 2007). We did not encounter *Pseudocophotis* during our surveys, and its relationship to other draconines remains unknown. Nonetheless, MBH examined the holotype (RMNH 3872) and two additional specimens (RMNH 4933 and ZMA 15190) housed in the Naturalis Museum, Leiden. In addition to the prehensile tail, the manual subdigital lamellae of *Pseudocophotis sumatrana* have very low keels and some basal lamellae are almost completely smooth. Although keels are somewhat higher on the toes, the condition of the hands is clearly intermediate between the near absence of keels in *Lophocalotes* and high keels of other Draconinae. Although our preliminary molecular data (Shaney et al. 2016; Harvey et al. 2017b) point to *Dendragama* as the sister genus of *Lophocalotes*, these shared morphological traits of *Lophocalotes* and *Pseudocophotis* complicates the still-incomplete picture of draconine phylogeny.

The two species of *Lophocalotes* exhibit more pronounced sexual dimorphism than that shown by species of *Pseudocalotes* or *Dendragama* (Harvey et al. 2014, 2017a). To examine the often-antagonistic effects of natural and sexual selection on sexual dimorphism, researchers have found it useful to further categorize sexual dimorphism as sexual size dimorphism, ornamentation, and either concealed or exposed dichromatism (Stuart-Fox and Ord 2004). Most dimorphic characters of *L. achlios* fall into the first of these categories: males of this species attain a larger size, have hypertrophied jaw musculature, and have relatively longer tails, shanks, dorsal crest scales, and heads than females. Two characters of males could be characterized as ornaments: numerous nuchal crest scales and a high, thickened base of the tail. Two concealed dichromatic characters of *L. achlios* are tongue coloration and ventral color, whereas an exposed dichromatic character is dorsal pattern. Among agamids, evolution of sexual size dimorphism, ornaments, and concealed dichromatism are all positively correlated with habitat openness (Stuart-Fox and Ord 2004). When comparing *Lophocalotes* to sympatric *Pseudocalotes*, however, we observed the opposite trend. The deep-forest species *L. achlios* has more pronounced sexual size dimorphism than the edge-habitat species *P. cybelidermus* and *P. guttalineatus*. The unusual dimorphism in tongue coloration of *Lophocalotes* would also be predicted in species of open habitats rather than in deep forests.

The most useful diagnostic characters are also sexually dimorphic. A researcher trying to identify a male specimen of *Lophocalotes achlios* should rely on gular pattern and morphology of the nuchal crest scales, whereas coloration of the buccal epithelium should be used to identify females. When working with preserved specimens, the color characters are not visible. Thus, researchers will have to assess specimens for the meristic and mensural characters identified as interspecific differences in our comparisons section. In recent reviews of Sumatran *Pseudocalotes* and *Dendragama* (Harvey et al. 2014, 2017a,b), we found coloration of the buccal epithelium to be useful in diagnosing new species. However, the present study is the first where we have observed sexual dichromatism in coloration of the buccal epithelium.

At several localities, *Lophocalotes* occurs in microsympatry with *Dendragama* (Doria 1888; Hallermann et al. 2004; Kurniati 2009; Harvey 2017a). However, *Dendragama* appears to always occurs in larger numbers. Both genera occur only above 1000 m and their evolutionary histories have likely been shaped by orogeny of the Bukit Barisan Range and climatic fluctuations associated with glacial cycles. *Lophocalotes ludekingi* occurs in sympatry with *D. boulengeri*, whereas *L. achlios* occurs in sympatry with *D. australis*. Similar genetic distances between these species pairs (6.0–6.3% for *Lophocalotes* and 6.0–6.4% for *Dendragama*) provide evidence that the genera share a common evolutionary history. Currently, *Dendragama* contains more species (Harvey et al. 2017a) and extends further northwest than *Lophocalotes*. North of its type locality, we did not find *Lophocalotes*, even though we discovered multiple new populations of *Dendragama*. However, our field surveys did not find *Lophocalotes* at its type locality or on nearby Gunung Marapi, even though *D. boulengeri* was relatively abundant on these mountains.

We have provided more ecological data than is typically reported in articles that describe new species. We found numerous noxious prey, especially ants and millipedes, in the diet of *Lophocalotes achlios* and the species' dietary niche is relatively broad. Although diets of Sumatran agamids remain virtually unknown, the diet of *L. achlios* is similar to better studied draconines such as *Calotes* (Diong et al. 1994; Matyot 2004), *Draco* (Inger 1983), *Japalura* (Kuo et al. 2007; Norval et al. 2012), and *Sitana* (Pal et al. 2007), where ants are the most numerous food item. These studies also found millipedes in stomach contents of *Calotes* and *Japalura*, but at substantially lower frequencies than in *L. achlios*. Like most iguanians, the slow-moving arboreal *L. achlios* most likely relies on ambush predation and visual cues. This foraging mode is typical of iguanians and dates to their divergence from other squamates (Vitt and Pianka 2005). Some draconines such as *Calotes mystaceus* apparently

cannot detect prey odors (Cooper 1989) and similar inability in *Lophocalotes* might explain the noxious prey in its diet.

Not surprisingly, lizard taxa that are new to science are likely to contain new parasites. Ours is the first report of intestinal helminths in *Lophocalotes* and one of few reports of parasites from Sumatran lizards (Shine et al. 1998). The high prevalence of *Spinicauda* in our sample leaves little doubt that this relatively large intestinal nematode directly affects the ecology of its host. Without further data, however, we can only describe parasite load, which increases with host SVL (small juveniles in our sample were uninfected). Both the high coefficient of dispersion and high probability that parasite burdens follow a negative binomial distribution reveal an aggregated population structure where relatively few hosts have substantially higher parasite loads. Crofton (1971) argued that most helminths have aggregated population structures, and one review (Shaw and Dobson 1995) found aggregated population structures in 268 out of 269 host–parasite systems. Nonetheless, magnitude of the coefficient of dispersion (often referred to as the relationship of level of aggregation to parasite burden) is influenced by ecology of both the parasite and its host. In the *Lophocalotes–Spinicauda* system, the coefficient is intermediate in value (Shaw and Dobson 1995): much less than the high coefficients of trichostongylid nematodes with single host life cycles, but greater than the low values observed in many cestodes and acanthocephalans. Discovery of this host–parasite system raises many questions, such as: do any of the three small arboreal sympatric draconines also harbor this parasite? Does the new nematode or, perhaps an undiscovered sister species, occur in *L. ludekingi*? And, how does the parasite's aggregated population structure affect population structure of *L. achlios*?

Although long rare in collections, *Lophocalotes* is actually quite common in several protected forests on Sumatra. We hope that the questions raised in this discussion inspire more research on the biology of these charismatic endemic agamids of Sumatra's volcanoes.

**Acknowledgments.**—We are grateful to the Ministry of Research and Technology of the Republic of Indonesia, RISTEK, for coordinating permissions. S. Wahyono (RISTEK) assisted throughout the permit approval process. We are grateful to representatives of LIPI at the Museum Zoologicum Bogoriense for facilitating in-house study of specimens and export and field research permits, namely Boeadi, M. Amir, R. Ubaidillah, R.M. Marwoto, and H. Sutrisno. RISTEK and LIPI reviewed and approved our fieldwork in Indonesia and provided export permits for specimens to the United States for deposition at UTA. The Forestry Department of Indonesia kindly provided research permits for areas under their jurisdiction, Kerinci Seblat NP (Sungai Penuh), Bukit Barisan Selatan NP (Kabu Perahu, Kota Agung). We thank A. Susdjoto (BBTN Bukit Barisan Selatan, Kota Agung) and Ir. Hartanto (DITJEN PHKA, Jakarta) for help with forestry permits. W. Tri Laksono provided laboratory assistance at the MZB, and N. Widodo and Mr. Marwoto (Faculty of Mathematics and Natural Sciences, UB) provided logistical support. We also thank participants in the expeditions to Sumatra: G. Barraza (Broward College), I. Sidik, Farid, Syaripudin, W. Tri Laksono, and G. Pradana (MZB), U. Arifin, F. Alhadi, A.M. Kadafi, D.R. Wulandari, R. Darmawan, K.I. Nawie, A. Dharasa, and S. Pratassi (Universitas Brawijaya), and C. Franklin, K. O'Connell, G.C. Sarker, U. Smart, P. Thammachoti, and E. Wostl (UTA). For hosting MBH's visits to their institutions, and/or loan of specimens used in this research, we thank J. McGuire and C. Spencer (MVZ), E. Dondorp (RMNH), and J. Streicher and P. Campbell (BMNH). C. Franklin (UTA) kindly catalogued and mailed specimens to MBH. All specimens were collected, euthanized, and preserved following guidelines detailed in the ASIH pamphlet: Guidelines for Use of Live Amphibians and Reptiles in Field and Laboratory Research, 2nd edition, available at http://www.asih.org/publications. A National Science Foundation grant (DEB-1146324) to ENS and MBH funded this research.

## LITERATURE CITED

Ananjeva, N.B., M.E. Dilmuchamedov, and T.N. Matveyeva. 1991. The skin organs of some iguanian lizards. Journal of Herpetology 25:186–199.

Ananjeva, N.B., N.L. Orlov, Q.T. Nguyen, and R.A. Nazarov. 2007. A new species of *Pseudocophotis* (Agamidae: Acrodonta: Lacertilia: Reptilia) from central Vietnam. Russian Journal of Herpetology 14:153–160.

Anderson, R.M., and D.M. Gordon 1982. Processes influencing the distribution of parasite numbers within host populations with special emphasis on parasite-induced mortalities. Parasitology 85:373–398.

Avise, J.C., and R.M. Ball, Jr. 1990. Principles of genealogical concordance in species concepts and biological taxonomy. Oxford Survey in Evolutionary Biology 7:45–67.

Bleeker, P. 1860. Reptiliën van Agam. Natuurkundig tijdschrift voor Nederlandsch Indië / uitgegeven door de Natuurkundige Vereeniging in Nederlandsch Indië 1860:325–329.

Bliss, C.I., and R.A. Fisher. 1953. Fitting the negative binomial distribution to biological data. Biometrics 9:176–200.

Boulenger, G.A. 1885. Catalogue of the Lizards in the British Museum (Natural History). Volume 1. Geckonidae, Eublepharidae, Uroplatidae, Pygopodidae, Agamidae. British Museum, UK.

Boulenger, G.A. 1887. Note on some reptiles from Sumatra described by Bleeker in 1860. Annals and Magazine of Natural History 20:152.

Brooks, D.R., and J.R. Palmier. 1981. Six platyhelminths from Malaysian reptiles including *Paradistomoidella cerberi* n. g., n. sp. (Digenea: Dicrocoeliidae). Journal of Helminthology 55:39–43. DOI: https://doi.org/10.1017/S0022149X0002544X

Bursey, C.R., S.R. Goldberg, and M.B. Harvey. 2017. *Spinicauda sumatrana* sp. nov. (Nematoda: Heterakidae) from Ludeking's Crested Dragon, *Lophocalotes ludekingi* (Agamidae), from the Bukit Barisan Range of Sumatra. Acta Parasitologica 62:610–616. DOI: https://doi.org/10.1515/ap-2017-0074

Cooper, W.E., Jr. 1989. Absence of prey odor discrimination by iguanid and agamid lizards in applicator tests. Copeia 1989:472–478.

Crofton, H.D. 1971. A quantitative approach to parasitism. Parasitology 62:179–193.

de Queiroz, K. 1998. The general lineage concept of species, species criteria, and the process of speciation: A conceptual unification and terminological recommendations. Pp. 57–75 in Endless Forms: Species and Speciation (D.J. Howard and S.H. Berlocher, eds.). Oxford University Press, USA.

De Rooij, N. 1915. The Reptiles of the Indo-Australian Archipelago. I. Lacertilia, Chelonia, Emydosauria. E.J. Brill, The Netherlands.

Diong, C.H., L.M. Chou, and K.K.P. Lim. 1994. *Calotes versicolor*, the changeable lizard. Nature Malaysiana 19:46–54.

Doria, G. 1888. Note erpetologiche: Alcuni nuovi sauri raccolti in Sumatra dal Dr. O. Beccari. Annali del Museo Civico di Storia Naturale di Genova 2:646–652.

Günther, A. 1872. On the reptiles and amphibians of Borneo. Proceedings of the Zoological Society of London 1872:586–600, Plates XXXV–XL.

Hallermann, J., N.O. Orlov, and N. Ananyeva. 2004. Notes on distribution and colour pattern of the rare agamid lizard *Lophocalotes ludekingii* (*sic*) (Bleeker, 1860) in Sumatra (Indonesia). Salamandra 40:303–306.

Hammer, Ø., D.A.T. Harper, and P.D. Ryan. 2001. PAST: Paleontological statistics software package for education and data analysis. Palaeontologia Electronica 4:1–9.

Harvey, M.B., A. Hamidy, N. Kurniawan, K. Shaney, and E.N. Smith. 2014. Three new species of *Pseudocalotes* (Squamata: Agamidae) from southern Sumatra, Indonesia. Zootaxa 3841:211–238. DOI: https://doi.org/10.11646/zootaxa.3841.2.3

Harvey, M.B., K.A. O'Connell, E. Wostl, A. Riyanto, N. Kurniawan, E.N. Smith, and L.L. Grismer. 2016. Redescription *Cyrtodactylus lateralis* (Werner) (Squamata:Gekkonidae) and phylogeny of the prehensile-tailed *Cyrtodactylus*. Zootaxa 4107:517–540. DOI: https://doi.org/10.11646/zootaxa.4107.4.3

Harvey, M.B., K. Shaney, I. Sidik, N. Kurniawan, and E.N. Smith. 2017a. Endemic dragons of Sumatra's volcanoes: New species of *Dendragama* (Squamata: Agamidae) and status of *Salea rosaceum* Thominot. Herpetological Monographs 31:69–97.

Harvey, M.B., K. Shaney, A. Hamidy, N. Kurniawan, and E.N. Smith. 2017b. A new species of *Pseudocalotes* (Squamata: Agamidae) from the Bukit Barisan Range of Sumatra with an estimation of its phylogeny. Zootaxa 4276:215–232. DOI: https://doi.org/10.11646/zootaxa.4276.2.4

Hubrecht, A.A.W. 1879. Contributions to the herpetology of Sumatra. Notes from the Leyden Museum 1:243–245.

Hubrecht, A.A.W. 1887. Tweede afdeeling. Kruipende dieren en visschen. Pp. 1–14 and Plates 1–3 in Midden-Sumatra. Reizen en Onderzoekingen der Sumatra-Expeditie, Uitgerust door het Aardrijkskundig Genootschap, 1877–1879, Beschreven door de Leden der Expeditie, onder Toezicht (P.J. Veth, ed.). E.J. Brill, The Netherlands.

Huelsenbeck, J.P., and F. Ronquist. 2001. MRBAYES: Bayesian inference of phylogeny. Bioinformatics 17:754–755.

Inger, R.F. 1983. Morphological and ecological variation in the flying lizards (genus *Draco*). Fieldiana Zoology 18:1–33.

Kearse, M., R. Moir, A. Wilson, ... A. Drummond. 2012. Geneious Basic: An integrated and extendable desktop software platform for the organization and analysis of sequence data. Bioinformatics 28:1647–1649. DOI: https://doi.org/10.1093/bioinformatics/bts199

Kuo, C.-Y., Y.-S. Lin, and Y.K. Lin. 2007. Resource use and morphology of two sympatric *Japalura* lizards (Iguania: Agamidae). Journal of Herpetology 41:713–723.

Kurniati, H. 2009. Herpetofauna diversity in Kerinci Seblat National Park, Sumatra, Indonesia. Zoo Indonesia, Jurnal Fauna Tropika 18:45–68.

Lanfear, R., B. Calcott, S.Y.W. Ho, and S. Guindon. 2012. PartitionFinder: Combined selection of partitioning schemes and substitution models for phylogenetic analyses. Molecular Biology and Evolution 29:1695–1701. DOI: https://doi.org/10.1093/molbev/mss020

Manthey, U., and W. Denzer. 2000. Description of a new genus, *Hypsicalotes* gen. nov. (Sauria: Agamidae) from Mt. Kinabalu, North Borneo, with remarks on the generic identity of *Gonocephalus schultzewestrumi* Urban, 1999. Hamadryad 25:13–20.

Manthey, U., and W. Grossmann. 1997. Amphibien und Reptilien Südostasiens. Natur und Tier Verlag, Germany.

Matyot, P. 2004. The establishment of the crested tree lizard, *Calotes versicolor* (Daudin, 1802) (Squamata: Agamidae), in Seychelles. Phelsuma 12:35–47.

Miralles, A., and M. Vences. 2013. New metrics for comparison of taxonomies reveal striking discrepancies among species delimitation methods in *Madascincus* lizards. PLoS One 8:e68242. DOI: https://doi.org/10.1371/journal.pone.0068242

Miralles, A., J. Köhler, F. Glaw, and M. Vences. 2016. Species delimitation methods put into taxonomic practice: Two new *Madascincus* species formerly allocated to historical species names (Squamata, Scincidae). Zoosystematics and Evolution 92:257–275. DOI: https://doi.org/10.3897/zse.92.9945

Norval, G., S.-C. Huang, J.-J. Mao, S.R. Goldberg, and K. Slater. 2012. Additional notes on the diet of *Japalura swinhonis* (Agamidae) from southwestern Taiwan, with comments about its dietary overlap with the sympatric *Anolis sagrei* (Polychrotidae). Basic and Applied Herpetology 26:87–97.

Pal, A., M.M. Swain, and S. Rath. 2007. Seasonal variation in the diet of the Fan-throated Lizard, *Sitana ponticeriana* (Sauria: Agamidae). Herpetological Conservation and Biology 2:145–148.

Pianka, E.R. 1973. The structure of lizard communities. Annual Review of Ecology and Systematics 4:53–74.

Pianka, E.R. 1986. Ecology and Natural History of Desert Lizards. Princeton University Press, USA.

Rohland, N., and D. Reich. 2012. Cost-effective, high throughput DNA sequencing libraries for multiplex target capture. Genome Research 22:939–946.

Sabaj, M.H. 2016. Standard Symbolic Codes for Institutional Resource Collections in Herpetology and Ichthyology: An Online Reference, Version 6.5. Accessed on 16 August 2016. Available at http://www.asih.org/. American Society of Ichthyologists and Herpetologists, USA. Archived by WebCite at http://www.webcitation.org/6vaNKqzcx on 9 December 2017.

Shaney, K.J., E. Wostl, A. Hamidy, N. Kurniawan, M.B. Harvey, and E.N. Smith. 2016. Conservation challenges regarding species status assessments in biogeographically complex regions: Examples from overexploited reptiles of Indonesia. Oryx 2016:1–12. DOI: https://doi.org/10.1017/S0030605316000351

Shaw, D.J., and A.P. Dobson. 1995. Patterns of macroparasite abundance and aggregation in wildlife populations: A quantitative review. Parasitology 111:S111–S133.

Shine, R., Ambariyanto, P.S. Harlow, and Mumpuni. 1998. Ecological traits of commercially harvested water monitors, *Varanus salvator*, in northern Sumatra. Wildlife Research 25:437–447.

Simpson, E.H. 1949. Measurements of diversity. Nature 163:688.

Smart, U., G.C. Sarker, U. Arifin, M.B. Harvey, I. Sidik, A. Hamidy, N. Kurniawan, and E.N. Smith. 2017. A new genus and two new species of arboreal toads from the highlands of Sumatra with a phylogeny of Sundaland toad genera. Herpetologica 73:63–75.

Stamatakis, A. 2006. RAx/ML-VI-HPC: Maximum likelihood-based phylogenetic analyses with thousands of taxa and mixed models. Bioinformatics 22:2688–2690.

Stuart-Fox, D.M., and T.J. Ord. 2004. Sexual selection, natural selection and the evolution of dimorphic coloration and ornamentation in agamid lizards. Proceedings of the Royal Society London 271:2249–2255.

Tamura, K., D. Peterson, N. Peterson, G. Stecher, M. Nei, and S. Kumar. 2011. MEGA5: Molecular evolutionary genetics analysis using maximum likelihood, evolutionary distance, and maximum parsimony methods. Molecular Biology and Evolution 28:2731–2739. DOI: https://doi.org/10.1093/molbev/msr121

Vitt, L.J., and E.R. Pianka. 2005. Deep history impacts present-day ecology and biodiversity. Proceedings of the National Academy of Sciences 102:7877–7881.

Wiens, J.J., and T.A. Penkrot. 2002. Delimiting species using DNA and morphological variation and discordant species limits in spiny lizards (*Sceloporus*). Systematic Biology 51:69–91.

Zug, G.R., H.H.K. Brown, J.A. Schulte II, and J.V. Vindum. 2006. Systematics of the garden lizards, *Calotes versicolor* group (Reptilia, Squamata, Agamidae), in Myanmar: Central dry zone populations. Proceedings of the California Academy of Sciences 57:35–68.

**Accepted on** 8 September 2017
**Associate Editor:** Bryan Stuart

## Appendix

### Specimens Examined

*Lophocalotes ludekingi* (14). INDONESIA: Jambi: trail up Gunung Kerinci, 1.72623–1.74717°S, 101.25914–101.26337°E, 1762–2292 m (MZB 14044, UTA 62841–62847, 62849); trail to Danau Tujuh, 1.7864°S, 101.3697°E, 1535 m (UTA 62850); trail to Danau Tujuh, 1.70974°S, 101.37089°E, 1529 m (UTA 62848). Sumatera Barat: Gunung Singgalang (BMNH 1946.8.24.38, holotype), Gunung Marapi 0.39424°S, 100.42395°E (MVZ 271740); Gunung Marapi, 0.39455°S, 100.42458°E (MVZ 271741).